Asteroid deflection by leveraging rotational self-energy

Andrea Viale *, Colin McInnes †, Gilles Bailet ‡ and Matteo Ceriotti §
University of Glasgow, Glasgow, G12 8QQ, Scotland, United Kingdom

A novel concept for the deflection of rotating asteroids is presented, based on the conversion of the asteroid rotational kinetic energy into translational kinetic energy. Such conversion is achieved using an orbital siphon, a tether-connected chain of masses, arranged vertically from the asteroid surface, which exploits the rotation of the asteroid for the delivery of mass from the asteroid to escape. Under the conditions to be discussed, the siphon can be initiated to ensure self-sustained flow of mass from the asteroid to escape. This mechanism is proposed to use a fraction of the asteroid as reaction mass, with the asteroid rotational kinetic energy leveraged to deliver the mass to escape and hence impart a reaction on the asteroid itself. Key parameters, such as velocity change, deflection duration, tension requirements and siphon length, are discussed. Deflection effectiveness is assessed for different release strategies. It is shown that typical velocity changes on the order of 1 cm s^{-1} can be achieved within a time window of a decade.

Nomenclature

G	gravitational constant
M	primary mass
m	secondary mass
R	primary radius
r	secondary radius
ω	angular velocity
ω_c	critical angular velocity
D	distance between primary and secondary center-of-mass
L	siphon length
L_{eq}	siphon equilibrium length
τ	tether tension

*Ph.D. Candidate. James Watt School of Engineering; a.viale.1@research.gla.ac.uk
†James Watt Chair, Professor of Engineering Science. James Watt School of Engineering; colin.mcinnes@glasgow.ac.uk
‡Research associate. James Watt School of Engineering; gilles.bailet@glasgow.ac.uk
§Lecturer in Space Systems Engineering. James Watt School of Engineering; matteo.ceriotti@glasgow.ac.uk

I	inertia
v	siphon radial velocity
F	siphon radial force
μ	siphon linear density
ρ	asteroid density
x	distance from primary center-of-mass
t	time
Δv	velocity change
X, Y	CW coordinates
E	mechanical energy
U	gravitational energy
K	kinetic energy
Δm	secondary mass collected before release
Δt	time to collect Δm
m_f	total released mass
A	siphon cross section
Subscripts:	
$\square_b$	center-of-mass
$\square_0$	initial value
$\square_p$	primary
$\square_s$	secondary
Superscripts:	
$\bar{\square}$	non-dimensional variable
Abbreviations:	
SR	single release
MR	multiple release
CW	Clohessy-Wiltshire

I. Introduction

Interest in near-Earth asteroids has grown over the past decade for two main reasons. They are abundant in useful resources that could be exploited in the context of asteroid mining, revolutionizing the future of space exploration [1]. On the other hand, a fraction of the near-Earth asteroids have been classified as potentially hazardous, due to their close

approaches to the Earth. The threat posed by a catastrophic asteroid collision with the Earth has stimulated research on possible impact avoidance methods. Most proposed approaches are characterized by momentum exchange between the asteroid and a reaction mass, in order to alter the asteroid trajectory so that it will miss Earth. The most discussed deflection solutions include kinetic impactor, nuclear detonation, gravity tractor, ion-beam shepherd, asteroid thrusting, mass drivers, methods based on changes on the thermo-optical properties of the surface and tether-based methods.

The kinetic impactor method consists in impacting a spacecraft onto the asteroid surface [2]. Due to the small mass of the spacecraft with respect to the asteroid, the momentum exchanged is mainly due to the high relative velocity between the spacecraft and the target asteroid. Better performances can be achieved with impact from retrograde orbits, in terms of impact speed and required mass [3]. Deflection via nuclear detonation is achieved by a nuclear explosion at a given standoff distance from the asteroid surface. The explosion causes local ablation of the asteroid surface and the momentum due to the expelled ejecta induces a modification of the asteroid trajectory. This method has proven to be especially effective for large asteroids and short lead times [4]. However, possible fracturing of the asteroid may cause unwanted outcomes and, therefore, knowledge of the shape and composition of the asteroid is crucial for this method. Moreover, the use of nuclear detonation in space is still controversial [5]. With the gravity tractor technique, a spacecraft (or a spacecraft formation) hovers in proximity to the asteroid using low-thrust propulsion, causing an acceleration of the center-of-mass of the asteroid-spacecraft system [6]. The ion-beam shepherd concept perturbs the asteroid using a collimated beam of plasma [7]. A second propulsion system is required to offset the momentum transferred to the asteroid. For small asteroids (with a diameter smaller than 100 m) the required spacecraft mass is one order of magnitude smaller than the gravity tractor [7], whereas comparable performances is observed for asteroids larger than 2 km. With direct thrusting [8] the entire asteroid is turned into a spacecraft, with a set of thrusters positioned on the asteroid surface applying continuous thrust. This method requires that the asteroid is firstly de-spun, to avoid a periodic change of the applied force direction. Clearly, the required thrust level scales with the asteroid size, thus making this method suitable only for smaller asteroids. In Ref. [9] it is proposed to modify the thermo-optical properties of the asteroid using the Yarkovsky effect. This effect is caused by the anisotropic emission of photons which produces a slight force with magnitude proportional to the temperature contrast across the asteroid. Changing the albedo of the asteroid surface (e.g., by means of paints) changes the intensity of such acceleration. This method requires timescales on the order of 100 years to achieve significant deflections [9]. Another proposed deflection method is based on mass drivers [10]. In this case, material collected from the asteroid is used as a reaction mass to be accelerated and released to escape to induce a velocity change on the asteroid. A significant advantage of this method is that the reaction mass is provided *in situ* therefore significantly reducing the launched mass of the deflection system. Based on this concept, it is proposed in Ref. [11] to achieve deflection by multiple ejection of boulders from the asteroid. Another class of methods for deflection is based on the use of tethers. Reference [12] proposes to connect a long tether and ballast to the asteroid to alter the center-of-mass of the system and therefore its orbit. Diversion can be enhanced by cutting the tether at an

appropriate time after attachment to the asteroid [13].

The methods described can be divided into two main categories. Kinetic impactor and nuclear detonation are single-event deflection methods, as the entire momentum transfer is applied a single time. Although the intensity of the momentum transfer can be very large (such as in the nuclear detonation method), there is a single opportunity for the deflection: in case of failure (e.g., insufficient velocity change, unwanted asteroid fragmentation) a new mission has to be rescheduled. In contrast, all the other methods permit continuous corrections, even though they might require longer timeframes for implementation. Moreover, many of the proposed methods will likely require a large mass of propellant or reaction mass to be delivered from Earth.

A new deflection method is proposed here which can be adapted to be both single-event and multiple-event and uses asteroid material as reaction mass. The method is based on the conversion of the rotational kinetic energy of the asteroid into translational kinetic energy. This technique has its foundation on the orbital siphon concept, devised by Davis, and elaborated in Ref. [14]. The orbital siphon is a chain of tether-connected payloads (here, the asteroid material) arranged vertically from the surface of the asteroid equator. If the siphon is long enough, the centrifugal-induced forces on the chain due to the body's spin overcome the gravitational forces and a net *orbital siphon effect* is initiated [15–18]: new payloads can be connected to the chain while top payloads are released. The delivery of payloads from the anchoring position to orbit does not require any external work to be done, as the force needed to overcome the gravity of the body is provided by the asteroid rotational kinetic energy. Here, it is proposed to collect the material lifted by the siphon and use it as a reaction mass to be released to change the asteroid velocity. If material is raised to a sufficient altitude, its mechanical energy overcomes the threshold value required for escape, therefore simple release of the collected mass without any additional energy is sufficient to induce a variation of the asteroid velocity. As with other mass driver methods, this technique calls for robotic rovers to transfer asteroid material to the siphon. However this paper will not directly address the surface activities of such rovers, but rather will focus on the siphon operation and performances.

The main scope of this paper is therefore to investigate what are the conditions to maximize the change in velocity (e.g., length of the siphon, mass throughput, time window) depending on the physical characteristics of the asteroid, in particular its rotational period and its density, under simplifying assumptions.

The paper is structured as follows. The orbital siphon model is firstly introduced and key parameters to evaluate the siphon performance are derived, in particular siphon radial velocity, the siphon equilibrium configurations, the time required to lift an arbitrary amount of mass and the reduction of the asteroid angular velocity resulting from siphon operation. Then, criteria to assess asteroid deflection are discussed, in terms of velocity change Δv and displacement from the original orbit, under two different scenarios: single mass release and multiple mass release.

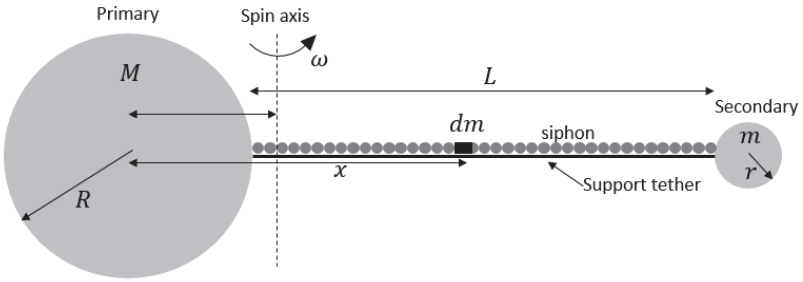

Fig. 1 Orbital siphon model.

II. Model

The system is composed of four main elements: the asteroid to be deflected (primary), the orbital siphon, the collected mass (secondary), and the support tether (Fig. 1). The asteroid is modelled as sphere with uniform density ρ, radius R, rotating with angular velocity ω, with the spin axis normal to the asteroid orbital plane. The secondary body is the material collected at the top of the siphon. It is assumed that the material is held together by a net-like or deformable structure which expands as material is collected. Detailed modelling of the secondary, including its shape, is outside the scope of this paper; here, for simplicity, the secondary is treated as a sphere.

A support tether connects the secondary to the primary and provides the necessary tension to prevent the secondary from escaping. The support tether is anchored at a point on the equator of the asteroid and it is assumed to be massless and inextensible.

The orbital siphon is the chain of tether-connected payloads that can slide without friction over the support tether. Here the mass of the tether connecting consecutive payloads is neglected and the total mass of the siphon is homogeneously spread over its length L. The siphon is therefore modelled as a continuous mass distribution with linear density μ.

Contrary to previous modelling approach as [15, 17], here the mass of the secondary is allowed to increase to non-negligible values, allowing the center-of-mass to be displaced significantly.

In general, the motion of the siphon will induce Coriolis forces, causing oscillations of the support tether in the equatorial plane [16]. However, it can be shown that if the mass of the secondary is (at least) two orders of magnitude larger than the mass of the siphon, then the torque generated by the centrifugal-induced force acting on the secondary counteracts the torque generated by the Coriolis force and it is reasonable to assume that the siphon is aligned with the local vertical. (see AppendixA). To justify the alignment between the siphon and the local vertical it can then be assumed that part of the secondary mass ($100\mu L$) is not used as reaction mass for the asteroid deflection but its instead retained as counterweight mass.

It is also assumed that the support tether and the secondary are within the gravitational sphere of influence of the

primary throughout the siphon operation. The radius of the sphere of influence of the asteroid is defined by [19]

$$r_{\mathrm{SOI}} \approx a \left(\frac{M}{M_{\odot}} \right)^{2/5} \tag{1}$$

where a is the semimajor axis of the asteroid orbit, M is the primary mass and $M_{\odot}$ is the the mass of the Sun. For a spherical body orbiting at one astronomical unit from the Sun, with a radius of 500 m the asteroid mass is $O(10^{12})$ kg, which yields a sphere of influence radius on the order of $O(10^4)$ m. As it will be shown, the typical siphon length requirements are smaller than this value, hence it is reasonable to assume that the secondary lies within the sphere of influence of the primary and Sun gravitational perturbation can be neglected.

A. Force on the siphon

Let M and m represent the primary and secondary mass at some point during siphon operation. Let dm be an infinitesimal element of mass of the siphon, x its distance from the primary and dx its length. Within an asteroid-fixed reference frame, the element dm is subjected to gravitational and centrifugal-induced forces. The gravitational force acting on dm can be written as:

$$dF_g = G \left(\frac{m}{(D-x)^2} - \frac{M}{x^2} \right) \mu dx \tag{2}$$

where $G = 6.67 \times 10^{-11}$ m^3 kg^{-1} s^{-2} is the gravitational constant and $D = R + L + r$ is the distance between primary and secondary center-of-mass. Note that the first positive component is due to the attraction towards the secondary, which enhances the siphon effect. Likewise, the centrifugal-induced force acting on the same mass element can be written as

$$dF_c = \omega^2 (x - x_b) \mu dx \tag{3}$$

where x_b is the distance between the center-of-mass of the system and the center of the primary:

$$x_b = \frac{mD}{M+m} \tag{4}$$

From this point, the subscript "0" appended to a variable represents the state of that variable at the beginning of siphon operation. Hence, for instance, R_0 and M_0 represent the initial radius and mass of the asteroid, respectively. The two forces can be written in non-dimensional form by scaling masses, distances and angular velocity by M_0, R_0 and $\sqrt{4/3G\pi\rho}$ respectively, giving:

$$d\bar{F}_g = \left(\frac{\bar{m}}{(\bar{D}-\bar{x})^2} - \frac{\bar{M}}{\bar{x}^2} \right) \bar{\mu} d\bar{x} \tag{5}$$

$$d\bar{F}_c = \bar{m}\bar{\omega}^2 (\bar{x} - \bar{D}) \bar{\mu} d\bar{x} \tag{6}$$

where the upper bar indicates a non-dimensional variable. The angular velocity scale factor corresponds to the rotational angular velocity of the asteroid at which gravitational and centrifugal-induced forces for a particle at the asteroid equator are balanced. As in previous work [15], this scale factor is called *critical angular velocity* and it is indicated with the symbol ω_c. Under the current assumption of a spherical asteroid, this parameter only depends on the asteroid density. For example, taking a density $\rho = 2\,\mathrm{g\,cm^{-3}}$ results in a critical period $2\pi/\omega_c = 2.3$ hours. If $\omega > \omega_c$ then material at the asteroid equator can be lifted to orbit or escape, unless cohesion is preventing particles from being displaced or the asteroid is a monolithic body [20]. Although only a small fraction of the known asteroid population is characterized by spin rates larger than the critical angular velocity [21], here $\omega > \omega_c$ is allowed for the sake of generality. The factor $\bar{\mu} = \mu/(4/3\pi R_0^2)$ can be interpreted as the ratio between the mass of the siphon and the asteroid mass, taking a siphon length $L = R_0$. The resulting force scaling factor is $M_0\omega_c^2 R_0$ (see Table 1 for a list of scale factors used in this paper). Then, the total force acting on the siphon is the integral

$$\bar{F} = \int_{\bar{R}}^{\bar{R}+\bar{L}} (d\bar{F}_g + d\bar{F}_c) \tag{7}$$

which admits the solution:

$$\bar{F} = \bar{\mu}\left[\frac{\bar{L}(1-\bar{R}^3)^{2/3}}{\bar{L}+(1-\bar{R}^3)^{1/3}} - \frac{\bar{L}\bar{R}^2}{\bar{L}+\bar{R}} + \frac{1}{2}\bar{L}\left[\bar{L}+2\bar{R}+2(\bar{R}^3-1)(\bar{L}+\bar{R}+(1-\bar{R}^3)^{1/3})\right]\bar{\omega}^2\right] \tag{8}$$

Due to the continuous mass distribution hypothesis, the siphon is effectively treated as a rigid body and the force $\bar{F}$ is applied at its center-of-mass. Note that, Eq. (8) can also be written as a function of the secondary mass by applying the substitution

$$\bar{R} = (1-\bar{m})^{1/3} \tag{9}$$

where the mass is scaled by M_0. Equation (9) follows from the conservation of mass $\bar{M} + \bar{m} = 1$.

To enable siphon operation the force $\bar{F}$ must be positive, i.e., directed towards the secondary:

$$\bar{F} > 0 \tag{10}$$

The siphon length $\bar{L}_{eq}$ that leads to $\bar{F} = 0$ is the *equilibrium length* and corresponds to the minimum length to guarantee the siphon effect. Figure 2 shows the equilibrium length as a function of the asteroid angular velocity $\bar{\omega}_0$ and the secondary mass $\bar{m}$. The black curve, corresponding to the case $\bar{m} = 0$ is the same equilibrium curve found in [15] for a siphon without a secondary mass. It is apparent from Fig. 2 that a larger secondary mass decreases the equilibrium length for a given angular velocity. Note that if $\bar{m} = 0.5$, the condition $\bar{F} = 0$ is verified for any $\bar{L}$. In fact, the condition $\bar{m} = 0.5$ implies that the system is symmetric with respect to its rotation axis.

Table 1 Scale factors for non-dimensional variables

Scale factors	
Distance	R_0
Mass	M_0
Time	ω_c^{-1}
Angular velocity	ω_c
Velocity	$\omega_c R_0$
Force	$M_0 \omega_c^2 R_0$

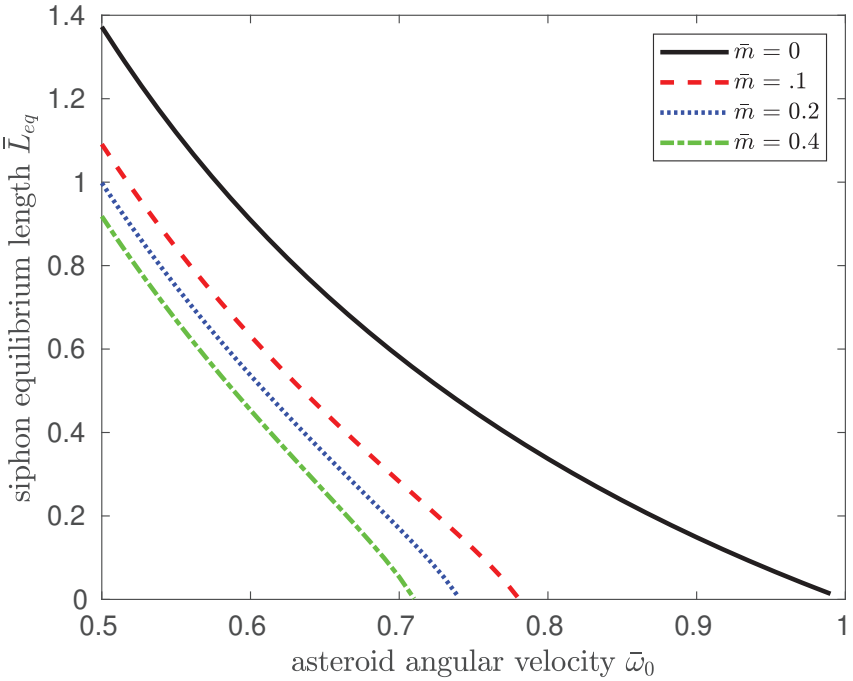

Fig. 2 Siphon equilibrium length as a function of the angular velocity for a range of secondary masses.

B. Support tether tension

The tension on the support tether can be found by considering the equilibrium of the forces at one of its ends. It must be stressed that here the support is modelled as a massless, inextensible tether and therefore its tension is constant over its length. The equilibrium of forces acting on the anchor point of the primary can be written as (the same result is obtained by considering the equilibrium on the attachment to the secondary):

$$M\omega^2 x_b - G\frac{Mm}{D^2} - \tau = 0 \tag{11}$$

where the tension force τ is considered positive when the tether is in tension. The first term appearing in Eq. (11) is the centrifugal-induced force due to the rotation of the primary with respect to the center-of-mass of the system and the second term is the gravitational attraction between the primary and the secondary. Clearly, a larger angular velocity will increase the tension in the tether, whereas a larger gravitational attraction between the primary and the secondary will reduce it. Solving Eq. (11) for τ and dividing both sides by the force scale factor (see Table 1), the resulting non-dimensional tension becomes:

$$\bar{\tau} = \bar{m}(1-\bar{m})\left(\bar{\omega}^2\bar{D} - \frac{1}{\bar{D}^2}\right) \tag{12}$$

The condition $\tau > 0$ must be verified to ensure the tether is always in tension. Such a requirement can be translated into a lower bound for the angular velocity:

$$\bar{\omega} > \sqrt{\frac{1}{\bar{D}^3}} \tag{13}$$

It will be shown that Eq. (13) is a necessary condition to enable insertion of the secondary mass to escape.

C. Conservation of angular momentum

If the inequalities (10) and (13) are verified, material is transferred from the primary to the secondary. Conservation of angular momentum can be invoked to evaluate the variation of angular velocity of the system in response to the transfer of a given amount of mass Δm from the primary to the secondary. Then, let the subscripts 1 and 2 refer to a variable *before* and *after* the transfer of material, respectively. Neglecting the mass of the siphon, the inertia of the system in the two states can be written as:

$$I_i = \frac{2}{5}(M_i R_i^2 + m_i r_i^2) + M_i x_{b,i}^2 + m_i(R_i + L + r_i - x_b)^2, \quad i = 1,2 \tag{14}$$

being

$$\begin{aligned} &M_1 = M; \quad M_2 = M - \Delta m; \\ &m_1 = m; \quad m_2 = m + \Delta m; \end{aligned} \tag{15}$$

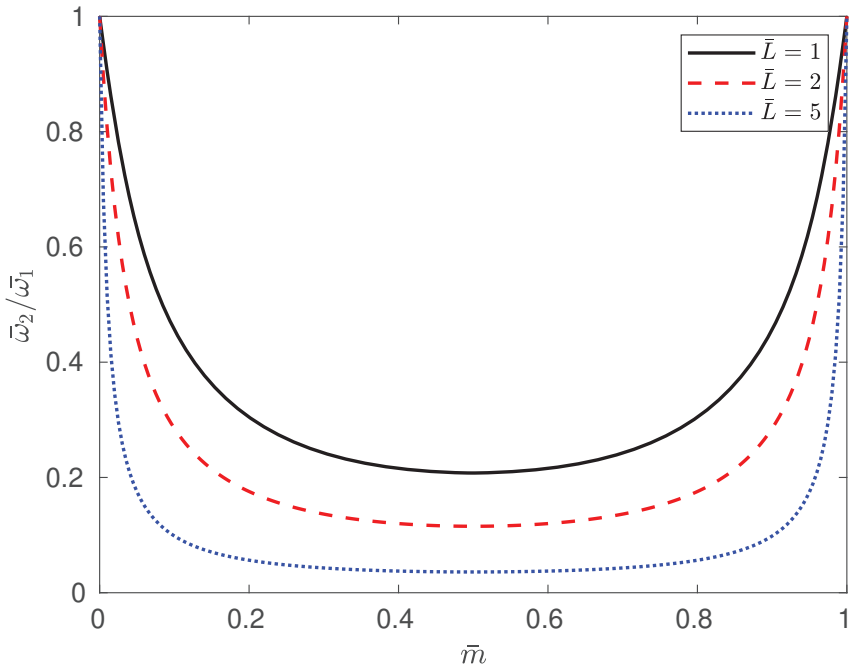

Fig. 3 Angular velocity ratio $\bar{\omega}_1/\bar{\omega}_2$ as a function of the secondary mass for a range of siphon lengths $\bar{L}$.

Note that R_i and $x_{b,i}$ can be written as a function of Δm through Eqs.(4) and (9). Conservation of angular momentum therefore requires that

$$I_1\omega_1 = I_2\omega_2 \tag{16}$$

Setting $M = M_0$, it follows $\Delta m = m$ and Eq. (16) can be further simplified and written in non-dimensional form:

$$\frac{\bar{\omega}_2}{\bar{\omega}_1} = \frac{2}{5\left(\bar{m}(1-\bar{m})\left(L + \bar{m}^{1/3} + (1-\bar{m})^{1/3}\right)^2 + \frac{2}{5}\left(\bar{m}^{5/3} + (1-\bar{m})^{5/3}\right)\right)} \tag{17}$$

Equation (17) describes the variation of the angular velocity of the system from the initial condition $\bar{M}_1 = 1$, $\bar{m}_2 = 0$ to the final condition $\bar{M}_2 = 1 - \bar{m}$, $\bar{m}_2 = \bar{m}$ as a function of the secondary mass. Note that, if the secondary mass is small ($m \to 0$), linearization of Eq. (17) reduces to the angular velocity ratio found in [15] for an orbital siphon releasing material to orbit:

$$\frac{\bar{\omega}_2}{\bar{\omega}_1} \approx 1 - 5\left(\frac{1}{6} + 5L + \frac{L^2}{2}\right)\bar{m} \tag{18}$$

Figure 3 shows the angular velocity ratio $\bar{\omega}_2/\bar{\omega}_1$ as a function of the secondary mass $\bar{m} \in [0, 1]$ for a range of siphon lengths. As expected, the ratio strictly decreases for $\bar{m} \in [0, 0.5]$. Clearly, the plot is symmetric with respect to $\bar{m} = 0.5$, i.e., if the secondary mass could be increased beyond $M_0/2$, the system would recover its initial angular velocity ω_0 when the entire asteroid mass is transferred to the secondary.

Substituting Eq. (17) into Eq. (8) with $\omega_2 = \omega$ and $\omega_1 = \omega_0$ allows the change of the siphon force as a function of

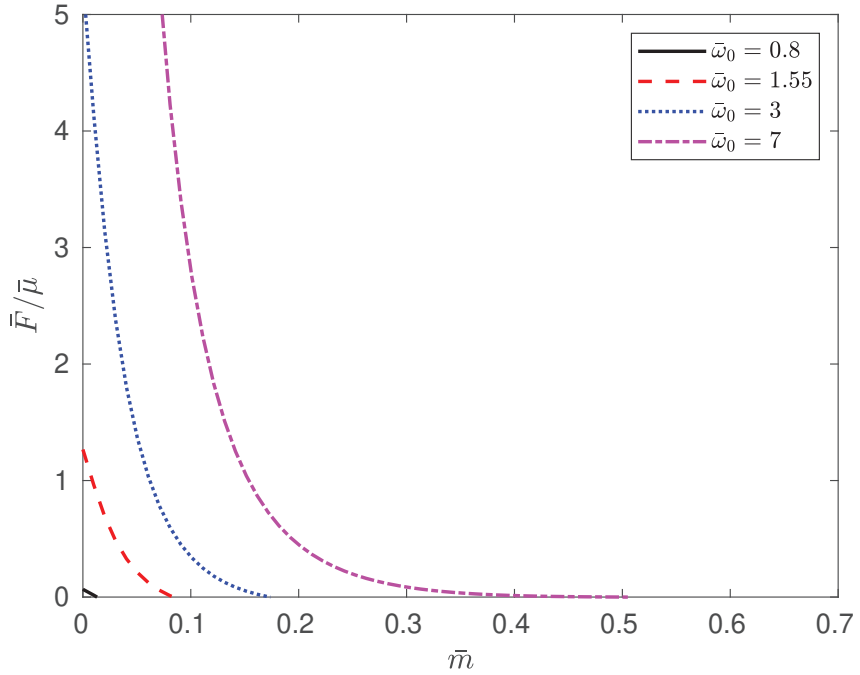

Fig. 4 Siphon force as a function of the secondary mass, for a range of initial angular velocities, taking $\bar{L} = 0.5$.

the asteroid initial angular velocity ω_0, the siphon length L and the extracted mass $\bar{m}$ to be seen. As an example, Fig. 4 shows the variation of the non-dimensional siphon force (here divided by $\bar{\mu}$) as a function of the secondary mass for a range of initial angular velocities $\bar{\omega_0}$ and taking $\bar{L} = 0.5$. When the siphon force is zero, the system has reached its equilibrium, thus arresting the siphon effect (unless the siphon length is changed, however variable length siphons are not consider here). Clearly, larger initial angular velocities permits the collection of a larger mass on the secondary. It can be verified that, if ω_0 is large enough to reach $\bar{m} = 0.5$, then $F < 0$, for any $\bar{m} \in [0.5, 1]$. Therefore, self sustaining mass flow from the primary to the secondary is not allowed for $\bar{m} > 0.5$.

D. Siphon operation and radial velocity

Siphon operation for a continuous mass distribution can be modelled by the three-step sequence shown in Fig. 5. If a net force $F > 0$ is acting on the siphon, it will accelerate in the direction of the secondary (from step (a) to step (b) in Fig.5). The term *radial velocity* will be used to indicate the velocity of the siphon with respect to the system barycentre. Upon raising by an infinitesimal amount $dx \approx 0$ a mass $dm = \mu dx$ is released to the secondary while an equal mass dm is connected at the bottom of the siphon (from step (b) to step (c) in Fig. 5. Let $dv_{ab} = v_b - v_a$ and $dv_{bc} = v_c - v_b$ be the change in siphon velocity from step (a) to (b) and from step (b) to (c) respectively, where v_a, v_b, v_c are the velocities of the siphon at step (a), (b) and (c) respectively. Then, the overall change in velocity dv_{ac} from step (a) to (c) can be written as:

$$dv_{ac} = dv_{ab} + dv_{bc} \tag{19}$$

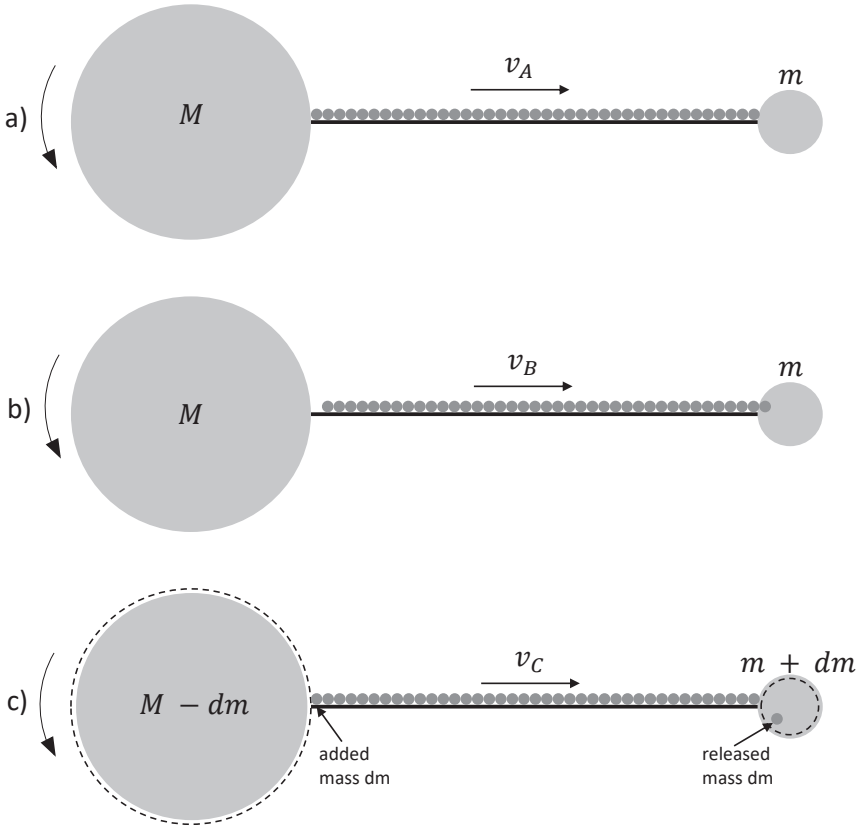

Fig. 5 Siphon operation sequence

The sequence is then iteratively repeated.

In the following, the values of dv_{ab} and dv_{bc} will be found by invoking the work-energy theorem and the conservation of linear momentum.

- From step (a) to step (b). The work per unit mass dW done by the gravitational and centrifugal-induced forces on the siphon to raise it by the amount dx is by definition:

$$dW = \frac{F}{\mu L} dx \tag{20}$$

Moreover, from the work-energy theorem:

$$dW = \frac{(v_a + dv_{ab})^2}{2} - \frac{v_a^2}{2} \tag{21}$$

By neglecting higher order terms and further simplifying, Eq. (21) can be written as:

$$dW = v_a dv_{ab} \tag{22}$$

Then, equating Eq. (20) and (22) yields:

$$dv_{ab} = \frac{F}{\mu L} \frac{dx}{v} \tag{23}$$

- From step (b) to step (c). The connection of the mass dm is modelled as an instantaneous inelastic collision. In reality, for siphons modelled as a discrete chain of tether connected payloads, each payload connection will cause some radial oscillations in the chain, that will be damped depending on the tether properties. However, it was shown in [15] that modelling the connection as an inelastic collision leads to similar equivalent result. Under this hypothesis the total linear momentum of the siphon is conserved between steps (b) and (c):

$$\mu L v_b = \mu dx v_b + \mu L v_c \tag{24}$$

Note that the first term on the right hand side is the momentum of the mass released to the secondary. Then, $dv_{bc} = v_c - v_b$ can be written as:

$$dv_{bc} = \frac{dx}{L} v_a \tag{25}$$

where the substitution $v_b = v_a + dv_{ab}$ is used and the higher order terms are neglected.

Substituting Eq. (23) and (25) into (19) yields:

$$dv_{ac} = \frac{F}{\mu L} \frac{dx}{v_a} - \frac{dx}{L} v_a \tag{26}$$

Dividing both sides by the infinitesimal time dt required to raise the siphon by dx and further simplifying yields

$$\frac{dv}{dt} + \frac{v^2}{L} = \frac{F}{\mu L} \tag{27}$$

where the subscripts have been removed. Equation (27) is the differential equation governing the radial velocity of a siphon modelled as a continuous mass distribution. Note the damping term proportional to the square of the siphon velocity. As a new mass element dm is added to the chain it must be accelerated to speed v. However, the rate at which new masses are being added scales as v, hence it can be shown that there is an apparent drag term which his quadratic in v.

Taking a siphon starting from $v(0) = 0$, Equation (27) admits the closed form solution:

$$v(t) = \sqrt{\frac{F}{\mu}} \tanh\left(\sqrt{\frac{F}{\mu}}\frac{t}{L}\right) \tag{28}$$

Using the non-dimensional scale factors in Table 1, Equation (28) can be written in non-dimensional form as:

$$\bar{v} = \sqrt{\frac{\bar{F}}{\bar{\mu}}} \tanh\left(\frac{\bar{t}}{\bar{L}/\sqrt{\bar{F}/\bar{\mu}}}\right) \tag{29}$$

Therefore, the siphon asymptomatically approaches the steady state radial velocity $\sqrt{F/\bar{\mu}}$. The transient behavior depends on the factor $\bar{L}/\sqrt{\bar{F}/\bar{\mu}}$ which represents the time required to reach 0.76% of the steady state velocity. For example, taking an asteroid with $\bar{\omega} = 0.85$, $\bar{L} = 1$ with $\bar{m} = 0$, the siphon reaches 76% of its asymptotic velocity after $\bar{t} = 1.3$ and 99% of its asymptotic velocity after $\bar{t} = 2.64$ corresponding to $t = 0.5$ h and $t = 1.3$ h respectively, for an asteroid with density $\rho = 2\,\mathrm{g\,cm^{-3}}$. As will be shown in the next sections, the time-scales required for siphon operation are on the order of years and therefore the effect of the transient can be reasonably neglected.

E. Timescale for mass transfer

The mass element dm released to the secondary in the time dt can be written as a function of the siphon linear density μ and the siphon velocity v:

$$dm = \mu v dt \tag{30}$$

To guarantee conservation of mass, if an element dm is released to the secondary, the primary mass must decrease by the same amount. For simplicity, it is assumed that the primary and the secondary retains spherical symmetry upon removal or release of mass, using the same approach as in Ref. [15]. Therefore, the removal of a mass element dm from

the primary implies the removal of its outer shell with radius dR such that:

$$dm = 4\rho\pi R^2 dR \tag{31}$$

Equating Eq. (31) and (30) and solving for dt yields:

$$dt = \frac{4\rho\pi R^2 dR}{\mu v} \tag{32}$$

Dividing both sides by the timescale factor ω_c^{-1} and noting that $d\bar{m} = \bar{R}^2 d\bar{R}$:

$$d\bar{t} = \frac{d\bar{m}}{\bar{\mu}\bar{v}} \tag{33}$$

Equation (33) can eventually be integrated to find the total time $\bar{t}$ required to increase the secondary mass from 0 to $\bar{m}_f$:

$$\bar{t} = \frac{1}{\bar{\mu}} \int_0^{\bar{m}_f} \frac{d\bar{m}}{\bar{v}} \tag{34}$$

where the siphon linear density is assumed constant during operation and therefore has been taken out from the integral. Neglecting the siphon radial velocity transient phase, $\bar{v} = \sqrt{\bar{F}/\bar{\mu}}$ (Eq. (29)). Then, using conservation of angular momentum, the integrand of Eq. (34) can be written as a function of $\bar{m}$, the initial angular velocity of the asteroid $\bar{\omega}_0$ and the siphon length $\bar{L}$. The resulting integral does not admit closed-form solution, therefore numerical integration must be used to evaluate an approximated solution.

III. Primary deflection

In this section the variation of the kinetic and potential energy of the system before and after detachment of the secondary from the support tether is considered, to study the fraction of rotational kinetic energy of the primary that can be converted into translational kinetic energy. Let E_0, E_-, E_+ and E_∞ represent the total energy of the system before the siphon operation starts (0), after collection of a mass m on the secondary (−), after release of mass m from the secondary (+) and, when the secondary has reached the sphere of influence of the primary after its release (∞).

The total energy of the system in the initial state 0 can be written as

$$E_0 = \frac{1}{2}\left(\frac{2}{5}M_0 R_0^2\right)\omega_0^2 - \frac{3}{5}\frac{GM_0^2}{R_0} \tag{35}$$

where the first term is the total rotational kinetic energy of the primary while the second term is the gravitational self-energy of the primary. Upon delivery of mass m to the secondary, the total energy becomes (neglecting the mass of

the siphon)

$$E_- = K_r^- + U_{self,p}^- + U_{self,s}^- + U_{mutual}^- \tag{36}$$

where K_r^- is the total rotational kinetic energy of the system (including primary and secondary), $U_{self,p}^-$ and $U_{self,s}^-$ are the gravitational self-energies of the primary and the secondary respectively whereas U_{mutual}^- is the mutual gravitational potential energy between two masses. The rotational kinetic energy can be written as:

$$K_r^- = \frac{1}{2}\left(\frac{2}{5}M^2R^2 + Mx_b^2 + \frac{2}{5}m^2r^2 + m(D-x_b)^2\right)(\omega^-)^2 \tag{37}$$

The angular velocity ω^- is obtained via conservation of angular momentum (Eq. (17)). The mutual gravitational potential U_{mutual}^- is:

$$U_{mutual}^- = -G\frac{Mm}{D} \tag{38}$$

It can be verified that $E_- - E_0 < 0$. In fact, part of the kinetic energy of material reaching the top of the siphon is lost due to the inelastic impact with the secondary.

Upon detachment of the secondary from the siphon, the primary and the secondary are released with velocity magnitudes Δv_p^+ and Δv_s^+, such that the total angular momentum before and after release is conserved:

$$\left(\frac{2}{5}MR^2 + Mx_b^2 + \frac{2}{5}mr^2 + m(D-x_b)^2\right)\omega^- = \frac{2}{5}MR^2\omega_p^+ + x_bM\Delta v_p^+ + \frac{2}{5}mr^2\omega_s^+ + (D-x_b)m\Delta v_s^+ \tag{39}$$

The angular momentum is evaluated with respect to the axis passing through the system center-of-mass and normal to the orbital plane. The variables ω_p^+ and ω_s^+ represent the angular velocity of the primary and the secondary after release. Eq. (39) is verified if

$$\omega_p^+ = \omega^- \tag{40a}$$

$$\omega_s^+ = \omega^- \tag{40b}$$

and

$$\Delta v_p^+ = \omega^- x_b \tag{41a}$$

$$\Delta v_s^+ = \omega^-(D-x_b) \tag{41b}$$

Equations (40a), (40b) dictate that the two bodies will spin about their respective center-of-mass with angular velocity ω^-, i.e., the same angular velocity about the system center-of-mass before release. The total energy of the system after

release is then:

$$E^+ = K^+_{r,p} + K^+_{r,s} + K^+_{t,p} + K^+_{t,s} + U^+_{self,p} + U^+_{self,s} + U^+_{mutual} \tag{42}$$

where

$$K_{r,p} = \frac{1}{2}\left(\frac{2}{5}MR^2\right)(\omega^+_p)^2, \quad K_{r,s} = \frac{1}{2}\left(\frac{2}{5}mr^2\right)(\omega^+_s)^2 \tag{43}$$

are the rotational kinetic energies of the primary and secondary after release respectively, and

$$K_{t,p} = \frac{1}{2}M(\Delta v^+_p)^2, \quad K_{t,s} = \frac{1}{2}m(\Delta v^+_s)^2 \tag{44}$$

are the corresponding translational kinetic energy. Substituting Eq. (40) and (41) into Eq. (42) yields $E_+ = E_-$, i.e., in absence of the energy losses during detachment, the total energy of the system is conserved.

Assuming two body dynamics after release, the total energy of the system is conserved. In particular, $E_\infty = E_+$. Since the rotational kinetic energies and self-energies of the two bodies play no role in the subsequent dynamical evolution of the system (their value is conserved and they cannot be further exchanged into other forms of energy within the system) let $E = E_+ - K^+_{r,p} - K^+_{r,s} - U^+_{self,p} - U^+_{self,s}$ be the sum of tranlsational kinetic energy and mutual potential upon release, which is conserved and regulates the subsequent orbital behavior of the two bodies. In particular, if $E > 0$ primary and secondary will have enough energy to escape each other. Conservation of the energy E from state + to ∞ yields:

$$\frac{1}{2}M(\Delta v^+_p)^2 + \frac{1}{2}m(\Delta v^+_s)^2 - G\frac{Mm}{D} = \frac{1}{2}M(\Delta v^\infty_p)^2 + \frac{1}{2}m(\Delta v^\infty_s)^2 \tag{45}$$

where Δv^∞_p and Δv^∞_s are the velocity magnitudes or the primary and the secondary with respect to the system center-of-mass when the two bodies are sufficiently far apart, i.e., at the the sphere of influence. The value Δv^∞_p represents the effective change in velocity imparted to the primary due to the release of m, taking into account the gravitational interaction between the two bodies within the sphere of influence. In order to solve Eq. (45) for Δv^∞_p, conservation of linear momentum is invoked *:

$$\Delta v^+_s = \frac{M}{m}\Delta v^+_p \tag{46}$$

Inserting Eq. (46), (41) and (4) into Eq. (45), after some algebraic manipulation, the magnitude of the primary hyperbolic escape velocity can be written in non-dimensional form as:

$$\Delta \bar{v}^\infty_p = \bar{m}\sqrt{(\bar{\omega}^+)^2\bar{D}^2 - \frac{2}{\bar{D}}} \tag{47}$$

As expected, Δv^∞_p is proportional to $\bar{m}$, suggesting that the collection of a larger secondary mass will increase the

*It is emphasized that Eq. (46) is relating the *magnitudes* of the velocities. From a vectorial point of view $\Delta \mathbf{v}_s = -\frac{M}{m}\Delta \mathbf{v}_p$. Note that Eq. (46) clearly holds also for Eqs. (41)

momentum exchange between the two bodies, thus contributing to a larger change in velocity of the primary. However, a larger $\bar{m}$ also implies a larger reduction of the asteroid angular velocity at release (Eq. (17)), thus reducing $\Delta\bar{v}_p^{\infty}$.

It is instructive to observe that the condition of secondary escape $E > 0$ can also be expressed as a lower bound for the angular velocity at release:

$$\bar{\omega} > \sqrt{\frac{2}{\bar{D}^3}} \tag{48}$$

where the superscript + has been removed from ω for simplicity. By comparing Eq. (48) and (13), it is apparent that the condition of secondary escape $E > 0$ is sufficient to guarantee positive tension of the support tether $\tau > 0$.

Moreover, by comparing Eq. (47) with (41a), the primary hyperbolic excess velocity can be written as a function of its release velocity:

$$\Delta\bar{v}_p^{\infty} = (\Delta\bar{v}_p)^{+}\left(1 - \frac{2}{\bar{D}^3\bar{\omega}^2}\right) \tag{49}$$

The factor $\frac{2}{\bar{D}^3\bar{\omega}^2}$ can be interpreted as a gravitational dragging coefficient, written as a function of the distance between the two bodies and the angular velocity of the system at release. When $\bar{D}^3\bar{\omega}^2 = 2$ (i.e., when $E > 0$, see Eq. (48)) $\Delta\bar{v}_p^{\infty} = 0$, and the secondary is inserted in bound motion around the primary.

Figure 6 shows in green the region of secondary escape ($E > 0$), as a function of $\bar{\omega}$ and $\bar{L}$, for $\bar{m} = 0$, $\bar{m} = 0.01$, $\bar{m} = 0.05$ and $\bar{m} = 0.12$. The orange region is associated with the secondary being inserted into a bound orbit around the primary $E < 0$. The red region represents the combination of $\bar{\omega}$ and $\bar{L}$ leading to an inverted mass flow, from the secondary to the primary ($F < 0$, Eq. (8)). For larger $\bar{m}$ the $E < 0$ region gradually shrinks and for $\bar{m} > 0.12$ the secondary can only be released to escape. The black contour on the $E > 0$ regions represents the value of the gravitational dragging factor. The black dotted line indicates the condition for zero tension on the support tether ($\tau = 0$, Eq. (11)). The region with $F > 0$ is also characterized by a positive support tether tension $\tau > 0$.

In the following sections, the superscript ∞ is removed and the hyperbolic excess velocity of the primary is simply indicated indicated with $\Delta\bar{v}_p$.

A. Upper bound for $\Delta\bar{v}_p$

It is instructive to observe that the velocity change of the primary $\Delta\bar{v}_p$ admits a theoretical upper bound due to energy conservation. In fact, assuming that the entire rotational kinetic energy could be converted into translational kinetic energy:

$$\frac{1}{2}\left(\frac{2}{5}M_0R_0^2\right)\omega_0^2 = \frac{1}{2}M_0\Delta v_{\max}^2 \tag{50}$$

where $\Delta v_{\max}$ is the maximum $\Delta\bar{v}_p$ achievable under these conditions and the term between brackets on the left hand side is the asteroid moment inertia. Then:

$$\Delta\bar{v}_{\max} = \sqrt{\frac{2}{5}}\bar{\omega}_0 \tag{51}$$

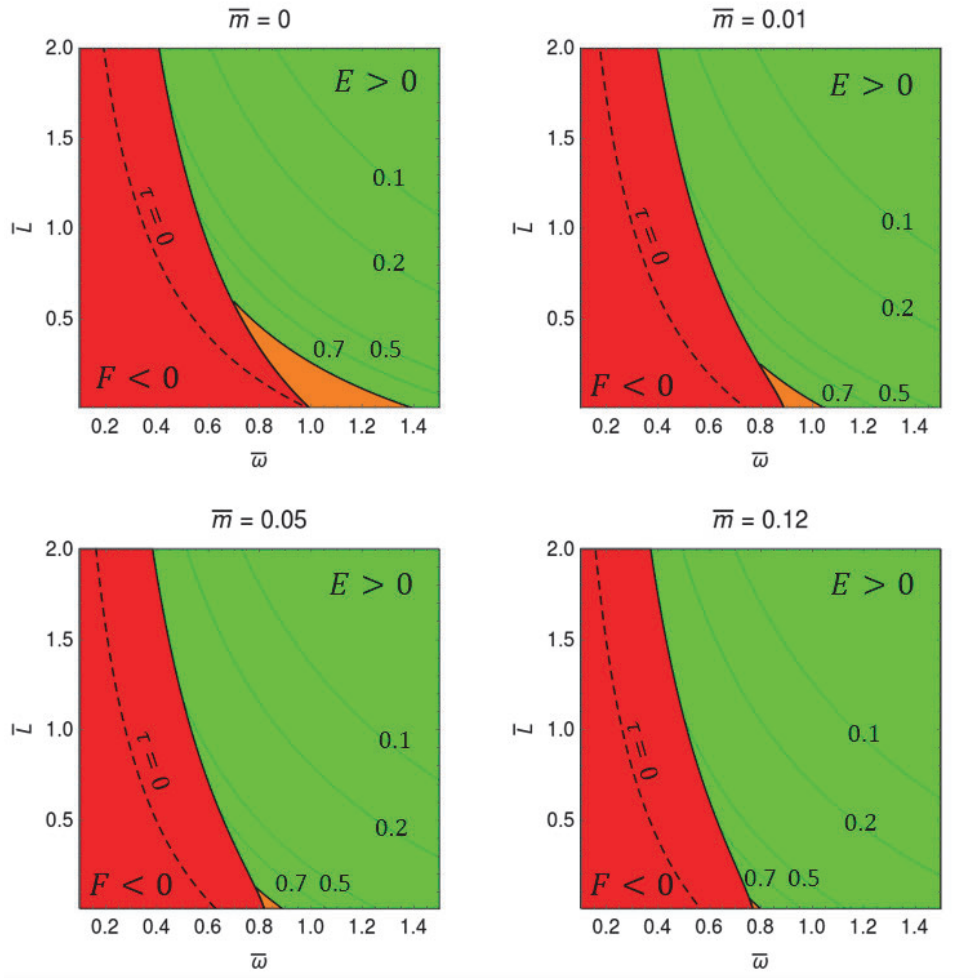

Fig. 6 Regions of secondary escape (green), release to bound orbit (orange) and siphon with negative force (red), as a function of the asteroid velocity $\bar{\omega}$ and the siphon length $\bar{L}$.

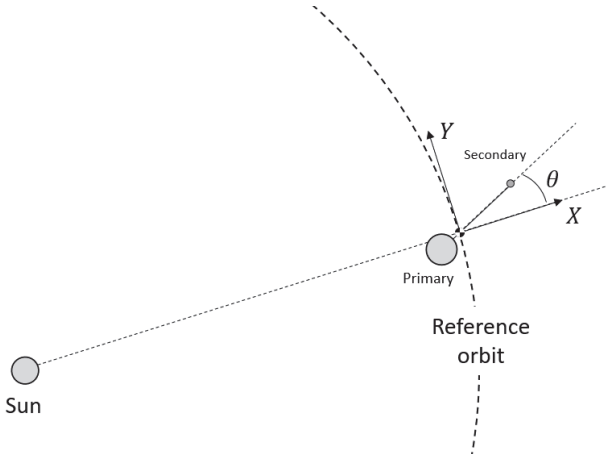

Fig. 7 CW reference frame.

For example, an asteroid with density $\rho = 2\,\mathrm{g\,cm^{-3}}$, radius $R_0 = 250\,\mathrm{m}$ and period 4 h admits a $\Delta\bar{v}_{\max} = 0.069\,\mathrm{m\,s^{-1}}$. This theoretical upper bound will be compared with Δv_p to assess the performance of the orbital siphon deflection.

B. Deflection distance

The Clohessy-Wiltshire (CW) equations [22] are used to assess the primary diversion achieved through release of the secondary mass. Here it is assumed that the initial heliocentric orbit of the primary is circular with zero inclination. The CW equations describe the motion of a chaser (in this case, the primary) with respect to a target reference frame (in this case, the unperturbed position of the primary before any manipulation occurs). Let $X - Y$ be a reference frame centered on the target with the X-axis parallel to the Sun-asteroid direction and the Y-axis in the direction of motion (Fig. 7). Let X_p, Y_p be the position of the primary in this frame and $\dot{X}_p, \dot{Y}_p$ its velocity. Analogous variables are defined for the secondary, with subscript s. Then, the CW equations for the two masses upon secondary release can be written as

$$\ddot{X}_i = 3n^2 X_i + 2n\dot{Y}_i + a_{i,X}, \quad i = p, s \tag{52a}$$

$$\ddot{Y}_i = -2n\dot{X}_i + a_{i,Y}, \qquad i = p, s \tag{52b}$$

where $n = 2\pi/T_{\mathrm{rev}}$, being T_{rev} the heliocentric orbit period of the asteroid, and $a_{i,X}, a_{i,Y}$ are the additional accelerations caused by the mutual gravitational interaction between the two masses. Here, the mutual gravitational terms are neglected and the primary is assumed to be released with the appropriate velocity magnitude at the sphere of influence (Eq. (47)). Thereby, Eqs. (52) can be solved in closed-form to find the state of the the primary as a function of time [22].

Using the scaling factors in Table 1:

$$\begin{pmatrix} \bar{X}_p(t) \\ \bar{Y}_p(t) \\ \dot{\bar{X}}_p(t) \\ \dot{\bar{Y}}_p(t) \end{pmatrix} = \begin{pmatrix} 4-3\cos\bar{n}\bar{t} & 0 & \frac{1}{\bar{n}}\sin\bar{n}\bar{t} & \frac{2}{\bar{n}}(1-\cos\bar{n}\bar{t}) \\ 6(\sin\bar{n}\bar{t}-\bar{n}\bar{t}) & 1 & \frac{-2}{\bar{n}}(1-\cos\bar{n}\bar{t}) & \frac{1}{\bar{n}}(4\sin\bar{n}\bar{t}-3\bar{n}\bar{t}) \\ 3\bar{n}\sin\bar{n}\bar{t} & 0 & \cos\bar{n}\bar{t} & 2\sin\bar{n}\bar{t} \\ -6n(1-\cos\bar{n}\bar{t}) & 0 & -2\sin\bar{n}\bar{t} & 4\cos\bar{n}\bar{t}-3 \end{pmatrix} \begin{pmatrix} \bar{X}_{0,p} \\ \bar{Y}_{0,p} \\ \dot{\bar{X}}_{0,p} \\ \dot{\bar{Y}}_{0,p} \end{pmatrix} \tag{53}$$

where $(\bar{X}_{0,p}, \bar{Y}_{0,p}, \dot{\bar{X}}_{0,p}, \dot{\bar{Y}}_{0,p})$ is the initial state of the primary. The parameter $\sqrt{\bar{X}_p(t)^2 + \bar{X}_s(t)^2}$ therefore represents the total diversion of the primary at the time t. As stated, it is assumed that $\sqrt{\dot{\bar{X}}^2 + \dot{\bar{Y}}^2} = \Delta v_p$. As regards the direction of the velocity vector and the position $X_{0,p}, Y_{0,p}$ it is assumed that: (i) the velocity at the sphere of influence is parallel to the release velocity and (ii) the position vector $(X_{0,p}, Y_{0,p})$ coincides with the release position. It will be shown that the primary trajectory resulting from these approximations does not differ significantly from that obtained by numerical integration of Eq. (52), thus making assumptions (i) and (ii) valuable approximations for this preliminary analysis. The primary release position is therefore completely defined by the angle θ between siphon and the X-axis. Here, it is chosen to release the secondary when $\theta = 0$ to ensure that the direction of Δv_p is parallel to the Y-axis, i.e., to the direction orbital motion. This changes the period of the resulting orbit and therefore increases the long-term drift with respect to the unperturbed path [10, 23]. Note that, using this model, $\theta = \pi$ would lead to an equivalent diversion trajectory, but symmetric with respect to the X-axis.

C. Diversion scenarios

Two diversion scenarios are considered: single (SR) and multiple (MR) secondary release. In the first case, a secondary mass Δm is collected at the secondary and released once. The secondary mass Δm and siphon length are selected in order to maximize the effective release velocity of the primary Δv_p. In the second case a smaller Δm (to be chosen) is collected and released multiple times, until the siphon reaches its equilibrium ($\bar{F} = 0$, Eq. (8)). The siphon length is chosen in order to maximize the total Δv_p, taken as the sum of the primary hyperbolic excess velocities at each release. In both cases the total deflection that can be achieved in a given time window t_{window} is calculated, for a given asteroid initial angular velocity $\bar{\omega}_0$, siphon linear density μ and heliocentric orbital period (that defines the parameter $\bar{n}$).

For a SR release scenario (see Fig. **??**):

1) The time Δt required to collect the secondary mass Δm is computed via Eq. (34).
2) If $\theta \neq 0$ at the end of mass collection the system rotates by an additional *phasing time* t_{phasing}, until the siphon is aligned with the X-axis of the CW frame.
3) If $\Delta t + t_{\text{phasing}} \geq t_{\text{window}}$, the siphon cannot raise the required secondary mass within the allocated time window

and the total displacement of the primary is zero. Similarly, if $\Delta t + t_{\text{phasing}} \leq t_{\text{window}}$ the secondary mass is released and the deflection is computed using Eq. (53).

The MR case is analogous, with steps 1 to 3 being iteratively repeated with the selected Δm, until the siphon reaches its equilibrium (see Fig. **??** for more details).

input: $\bar{\omega}_0, \bar{n}, \bar{\mu}$

output: deflection

begin

  $(X_p, Y_p, \dot{X}_p, \dot{Y}_p) = (0, 0, 0, 0)$;

  $\Delta t \leftarrow$ time to collect Δm ;

  if mod $(\theta, 2\pi) \neq 0$ **then**

    $t_{\text{phasing}} \leftarrow$ phasing time required to reach mod $(\theta, 2\pi) = 0$;

    $\Delta t = \Delta t + t_{\text{phasing}}$;

  end

  if $\Delta t < t_{window}$ **then**

    $(X_{0,p}, Y_{0,p}, \dot{X}_{0,p}, \dot{Y}_{0,p}) = (X_p, Y_p, \dot{X}_p, \dot{Y}_p) + (-x_b, 0, 0, v_{p,\infty})$;

    $(X_p, Y_p, \dot{X}_p, \dot{Y}_p) \leftarrow$*Eq.* (53) $\leftarrow (X_{0,p}, Y_{0,p}, \dot{X}_{0,p}, \dot{Y}_{0,p})$;

  end

  deflection $= \sqrt{X_p^2 + Y_p^2}$;

end

Fig. 8 Single Release deflection

As an example, Figures 10 shows the deflection trajectory in the CW frame for an asteroid with $\bar{\omega}_0 = 0.65$, $\bar{\mu} = 2.87 \times 10^{-7}$ (this corresponds to a siphon with linear density $150\,\text{kg}\,\text{m}^{-1}$ on an asteroid with radius 250 m) and $\bar{n} = 2.66 \times 10^{-4}$ (corresponding to an asteroid with density $\rho = 2000\,\text{kg}\,\text{m}^{-3}$ with orbital period of 1 year), for a SR (a) and MR case (b). For the SR, the total $\Delta\bar{m}$ that maximizes the primary release velocity is $\Delta\bar{m} = 0.027$. In the MR case, $\Delta m = 2 \times 10^{-3}$ is chosen. In each case, the initial part of the secondary trajectory is included for completeness.

Figures 11 shows the difference between the diversion trajectory calculated using Eq. (53) and by numerical integration of Eq. (52) taking into account the mutual acceleration terms. Note that the end points are very close in both cases. The same degree of accuracy can be verified by choosing different values of $\bar{\omega}_0$, $\bar{\mu}$ and $\bar{n}$.

IV. Results

Figure 12 shows the quantity of mass that can be collected at the secondary $\bar{m}_f$, given the siphon length $\bar{L}$ and the initial angular velocity of the primary $\bar{\omega}_0$. Each region represents the states $(\bar{m}_f, \bar{L})$ that can be reached for the indicated initial angular velocity intervals. For example, the point $(\bar{m}_f, \bar{L}) = (0.1, 1)$ lies within the region $\bar{\omega}_0 > 1$, meaning it is not possible to collect 10% of the initial asteroid mass if the primary is spinning below the critical angular velocity ($\bar{\omega}_0 = 1$). As expected, a larger initial angular velocity is needed to collect larger secondary masses. For an asteroid spinning at its critical angular velocity, ($\bar{\omega}_0 = 1$), the maximum mass fraction that can be collected at the

input: $\bar{\omega}_0, \bar{n}, \bar{\mu}$

output: deflection

begin

doIterate = True;

$(X_p, Y_p, \dot{X}_p, \dot{Y}_p) = (0, 0, 0, 0)$;

while *doIterate* **do**

$F_{\text{end}} \leftarrow$ siphon force after collection of Δm;

if $F_{end} < 0$ **then**

Reduce Δm such that $F_{\text{end}} = 0$;

doIterate = False;

end

$\Delta t \leftarrow$ time to collect Δm ;

if $\mod(\theta, 2\pi) \neq 0$ **then**

$t_{\text{phasing}} \leftarrow$ phasing time required to reach $\mod(\theta, 2\pi) = 0$;

$\Delta t = \Delta t + t_{\text{phasing}}$;

end

if $\Delta t < t_{window}$ **then**

$(X_{0,p}, Y_{0,p}, \dot{X}_{0,p}, \dot{Y}_{0,p}) = (X_p, Y_p, \dot{X}_p, \dot{Y}_p) + (-x_b, 0, 0, v_{p,\infty})$;

$(X_p, Y_p, \dot{X}_p, \dot{Y}_p) \leftarrow$*Eq.* (53) $\leftarrow (X_{0,p}, Y_{0,p}, \dot{X}_{0,p}, \dot{Y}_{0,p})$;

else

doIterate = False;

end

end

if $\Delta t < t_{window}$ **then**

$(X_{0,p}, Y_{0,p}, \dot{X}_{0,p}, \dot{Y}_{0,p}) = (X_p, Y_p, \dot{X}_p, \dot{Y}_p)$;

$(X_p, Y_p, \dot{X}_p, \dot{Y}_p) \leftarrow$*Eq.* (53) $\leftarrow (X_{0,p}, Y_{0,p}, \dot{X}_{0,p}, \dot{Y}_{0,p})$;

end

deflection = $\sqrt{X_p^2 + Y_p^2}$

end

Fig. 9 Multiple Release deflection

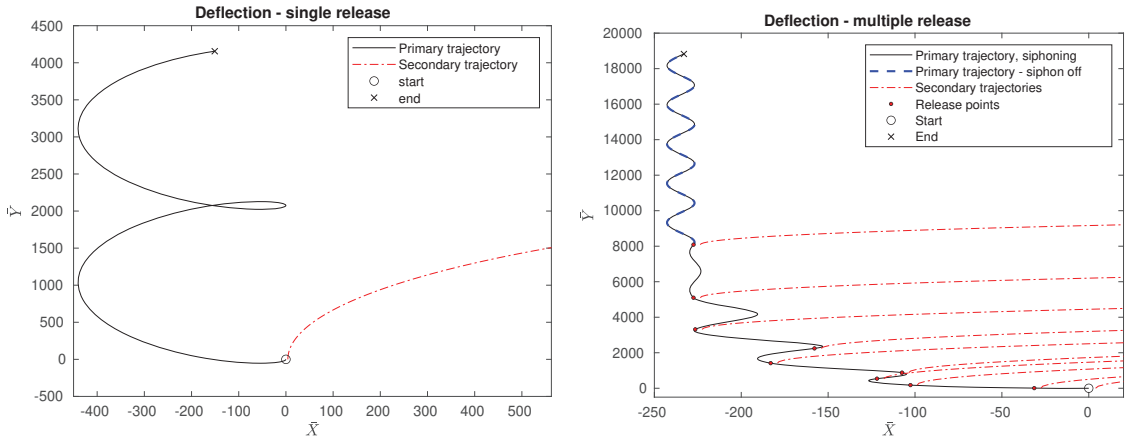

(a) (b)

Fig. 10 Single (a) and multiple (b) release deflection

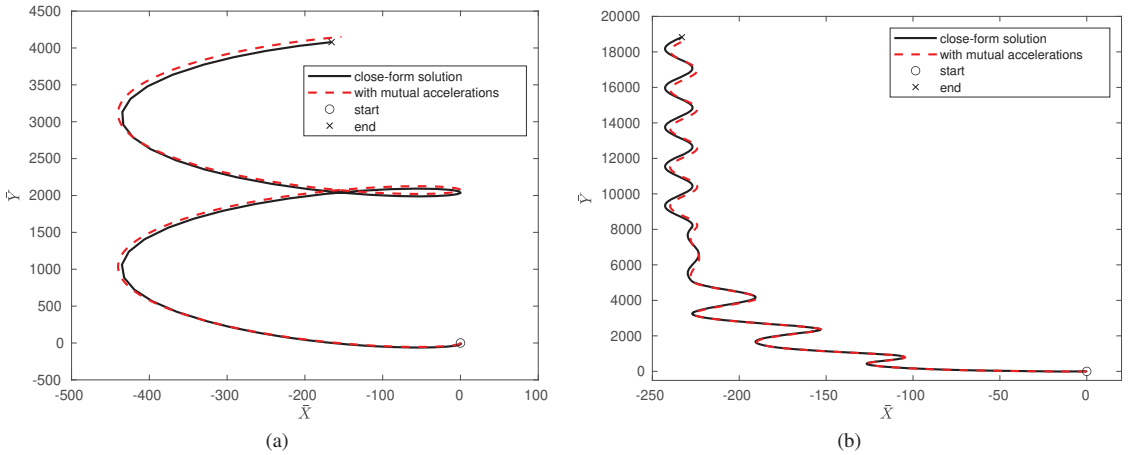

Fig. 11 Comparison between primary trajectory obtained using Eq. (53) **(black) with respect to numerical solution of Eq.** (52) **(red).**

secondary is $\bar{m}_f = 0.08$, which is consistent with the results found in Ref. [15]. The minimum angular velocity required for collecting half of the asteroid mass $\bar{m}_f = 0.5$ is approximately 1.56. Therefore, an asteroid should spin to more than 56% of its critical angular velocity to enable separation of half of its mass using the orbital siphon. Assuming an asteroid density of $\rho = 2\,\mathrm{g\,cm^{-3}}$ this is equivalent to a rotation period of 1.5 h.

Figure 13 shows the primary velocity change $\Delta\bar{v}_p$ as a function of the released secondary mass $\bar{m}_f$ and the siphon length for $\bar{\omega}_0 = 0.7$ (a), $\bar{\omega}_0 = 1.56$ (b), in a SR release scenario. In general, a larger secondary mass (and a larger siphon length) enables a larger $\Delta\bar{v}_p$, since the displacement between the primary and the system barycenter increases. At the same time, however, a larger secondary mass (or longer siphon) implies a lower angular velocity of the system $\bar{\omega}$ at the end of the siphon manipulation, thus increasing the gravitational dragging factor (see Eq. (49)). Then, the maximum $\Delta\bar{v}_p$ is a tradeoff between these two opposite effects and, in general, the siphon length required to maximize $\Delta\bar{v}_p$ does not match that required to maximize $\bar{m}_f$. For example, in the case $\bar{\omega}_0 = 1.56$, the siphon length needed to approach the half mass separation point ($\bar{m}_f = 0.5$) progressively decreases, thus increasing the gravitational dragging effect at release and reducing $\Delta\bar{v}_p$: the optimal $\Delta\bar{v}_p$ is reached for a siphon length $\bar{L} \approx 0.5$, with a total collected mass $\bar{m}_f = 0.22$.

The black and red contour show the non-dimensional time and maximum support tension respectively. Here $\bar{t}$ is multiplied by the factor $\bar{\mu}$ to eliminate dependence on the siphon linear density (see Eqs (34), (11)). As expected, both time and tension are maximized at the largest $\bar{m}_f$ allowed for the given $\bar{\omega}_0$.

Figure 14 compares $\Delta\bar{v}_p$ (a), time (b), total released mass (c) and final angular velocity (d) between SR and MR (taking $\Delta\bar{m} = 1 \times 10^{-4}$ for MR), in the condition of max $\Delta\bar{v}_p$. It is apparent that the MR scheme enables a larger velocity change in a shorter time. This is due to the fact that, by releasing smaller masses multiple times, rather than a single larger mass a single time, the gravitational dragging effect is reduced and, even though the total released mass is

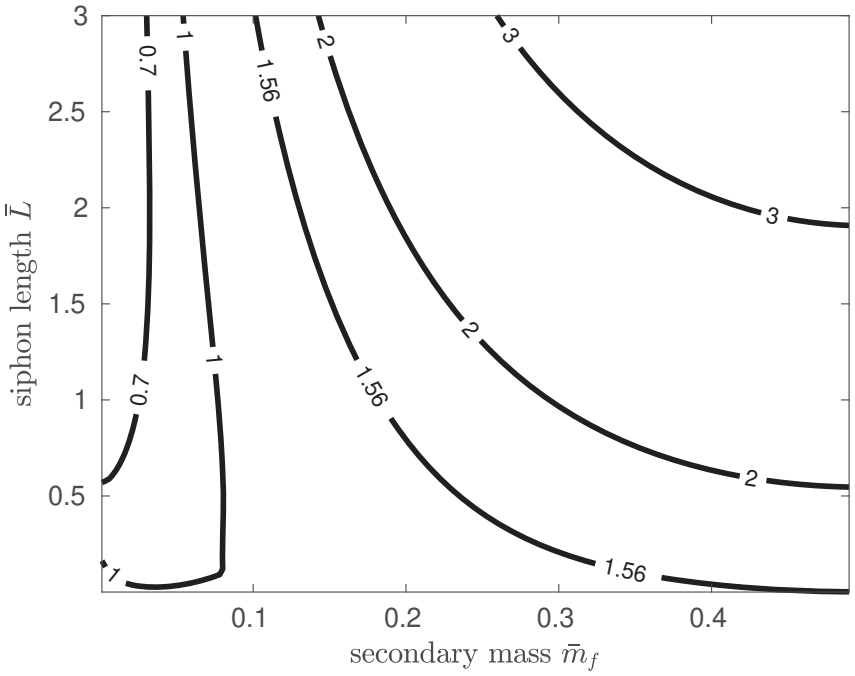

Fig. 12 Isocurves of asteroid initial angular velocity ω_0 as a function of the siphon length and the secondary mass.

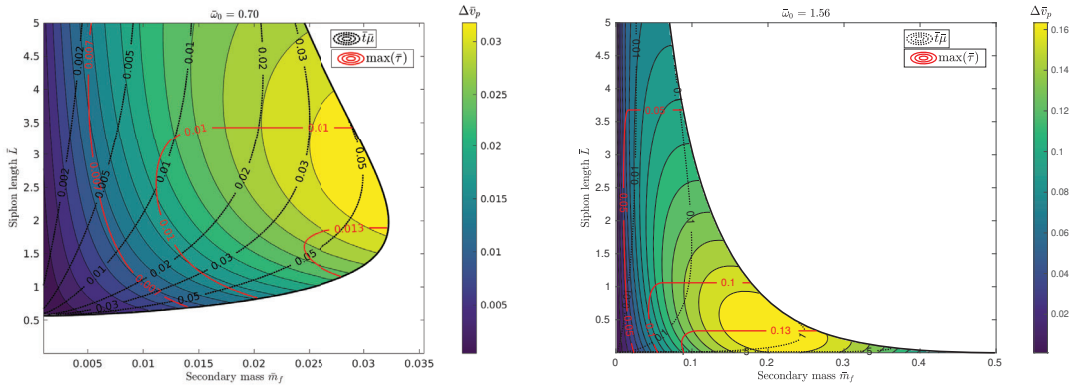

(a) (b)

Fig. 13 Primary release velocity (colored contour), time for mass transfer $\bar{t}\bar{\mu}$ and maximum tension τ as a function of the secondary mass $\bar{m}_f$ and the siphon length $\bar{L}$.

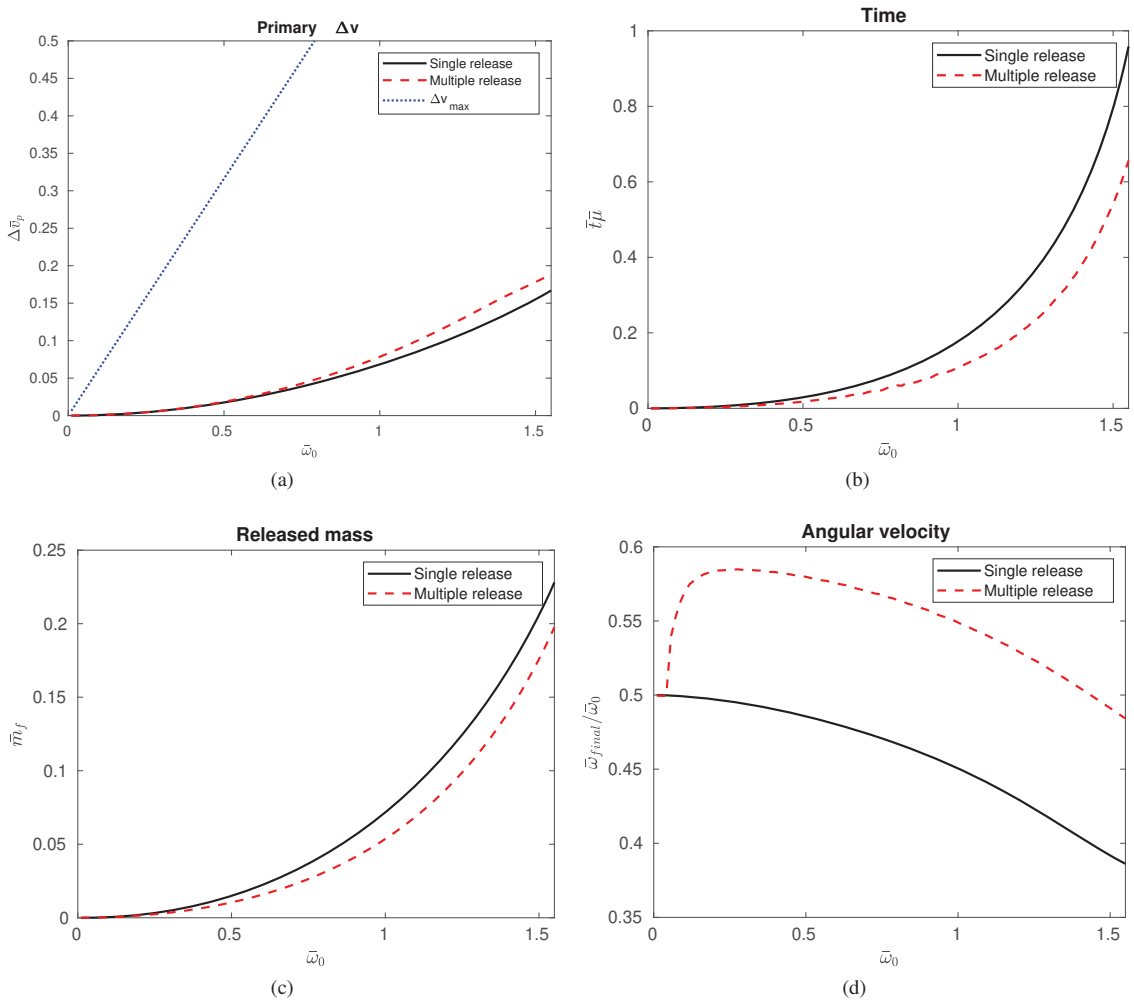

Fig. 14 Primary $\Delta\bar{v}$ (a), time (b), released mass (c) and siphon length (d) as a function of the asteroid non-dimensional angular velocity $\bar{\omega}_0$.

smaller in the MR case (Fig. 14c), the overall achievable $\Delta\bar{v}_p$ is larger. Note that, in both cases, Fig. 14(b) refers to the total time required to extract the mass shown in Fig. 14c. The blue dotted line in Fig. 14a represents $\Delta\bar{v}_{max}$ (Eq. (51)), i.e., the theoretical primary velocity change that would be obtained if the rotational kinetic energy of the asteroid could be entirely converted into transitional kinetic energy. For example, at $\bar{\omega}_0 = 1$ the $\Delta\bar{v}_p$ obtained by a SR siphon is only $0.11\Delta\bar{v}_{\max}$. This difference is due to two unavoidable limits of the proposed mechanism: the gravitational dragging at release, and the residual angular velocity of the asteroid at the end of the manipulation process (Fig. 14d). In particular, with a fixed length siphon, the asteroid will always retain a final non-zero rotational kinetic energy at the end of the release process, (between 40 and 60 percent of the initial angular velocity, depending on the release scenario and the initial angular velocity) that cannot be further exploited, since the siphon has reached its equilibrium state ($\bar{F} = 0$, Eq. (8)).

Figure 15 illustrates the dimensional values of the primary Δv_p (a), time (b), tension (c) and siphon length (d) as a function of the asteroid initial rotation period, taking an asteroid density $\rho = 2\,\mathrm{g\,cm^{-3}}$ with radius 250 m (black curves), and 500 m (red curves). Again, each plot refers to the condition of maximum Δv_p. For an asteroid with radius 250 m, Δv_p varies between 1.5 and $0.3\,\mathrm{cm\,s^{-1}}$ when its period ranges form 2.3 and 6 hours with the time requirements below 8 years. Note that, from the definition of the scale factors, $\Delta v_p \propto R_0$ and $t \propto R_0^2$. Therefore, although a larger Δv_p is permitted for larger asteroids, the time scale increases quadratically with the radius. Moreover, $\Delta v_p \propto \omega_c \propto \sqrt{\rho}$ and $t \propto \omega_{\mathrm{crit}}^{-1} \propto 1/\sqrt{\rho}$, i.e., a larger asteroid density increases the Δv of the primary while also increasing the time requirements. Figure 15c indicates that the support tether tension can vary by several orders of magnitude when comparing SR and MR methods. For example, an asteroid with radius $R_0 = 250\,\mathrm{m}$ requires a support tether tension $\tau = O(10^5)$ N for a SR case which drops to $O(10^3)$ N in a MR case. In general, τ increases with smaller rotational periods and this becomes more noticeable for a larger asteroid radius. Note from the force scaling that $\tau \propto M_0 \omega_c^2 R_0 \propto \rho^2 R_0^4$, hence the tension is strongly influenced by the asteroid density and its size. Figure 15d shows that the siphon length in the MR case is slightly smaller with respect to the SR case. Moreover, in both cases, L is smaller than the radius of the sphere of influence (represented with a dotted line in Fig. 15d) and, in general, it can be verified that this holds true even for larger asteroid radii. Therefore, the siphon is always within the sphere of influence of the asteroid thus justifying the choice of neglecting the solar gravitational perturbations in this preliminary analysis. Note that the asteroid density does not influence the siphon length required to maximize $\Delta \bar{v}_p$ and, from the distance scale factor, $L \propto R_0$.

Figure 16 shows the siphon linear density required to divert an asteroid by 1 Earth radius within a time window of 5 years (first row), 10 years (second row), 15 years (third row), as a function of the asteroid period, for a range of asteroid radii $R_0 = 250\,\mathrm{m}$ (first column), $R_0 = 500\,\mathrm{m}$ (second column), $R_0 = 1000\,\mathrm{m}$ (third column) , for SR case (black line) and MR case (with $\Delta \bar{m} = 5 \times 10^{-3}$ (red line) and $\Delta \bar{m} = 1 \times 10^{-4}$ (blue line)). The range of allowed μ has been limited to $2 \times 10^3\,\mathrm{kg\,m^{-1}}$, thus any scenario requiring a larger μ is not represented here. It is apparent that a MR scheme significantly reduces the minimum μ. Moreover, lower values of $\Delta \bar{m}$ further reduce the siphon linear density. For a fixed requirement on the total diversion, larger μ are needed in the SR case to increase the mass throughput to the secondary and achieve the required deflection within the given time window. At the same time, however, if the collected mass is too large, the gravitational dragging effect might reduce the overall $\Delta \bar{v}_p$. This explains why the minimum μ can significantly increase for shorter periods in the SR case. In general, lower values of siphon linear density are allowed for smaller asteroids. It is interesting to observe that for a given time window and radius there is an upper bound on the asteroid period at which $\mu \to \infty$. For example, it is impossible to deflect a 250 m by 1 Earth radius in 5 years if its initial period is longer then 3 hours (not even using an hypothetical siphon with infinite linear density). Such upper bounds on the asteroid period approaches the critical period (i.e., $2\pi/\omega_c$) for smaller asteroids.

Figure 17 shows the isocurves of minimum siphon linear density to deflect an asteroid by 1 Earth radius (black)

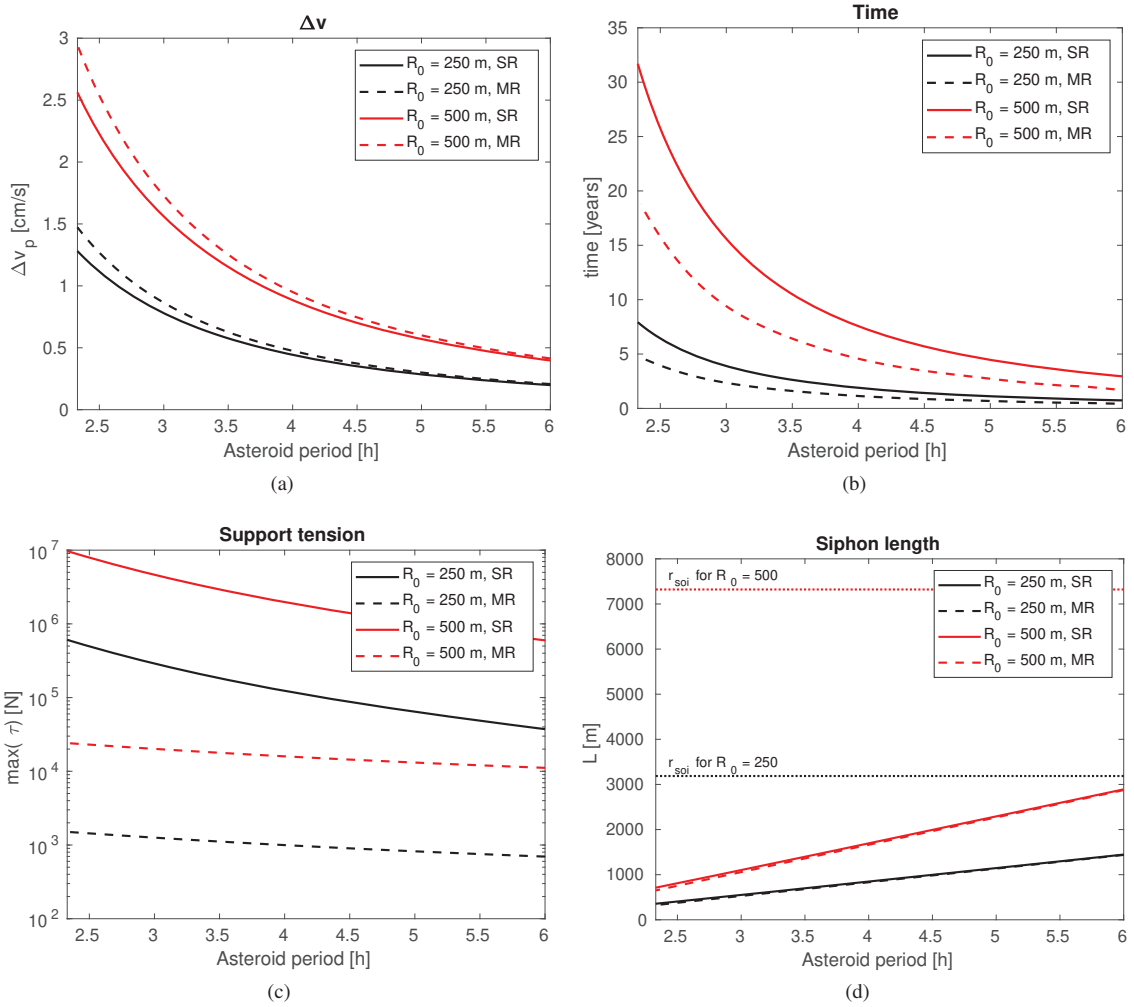

Fig. 15 Primary $\Delta\bar{v}_p$, time, support tether tension and siphon length as a function of the asteroid period, using dimensional units.

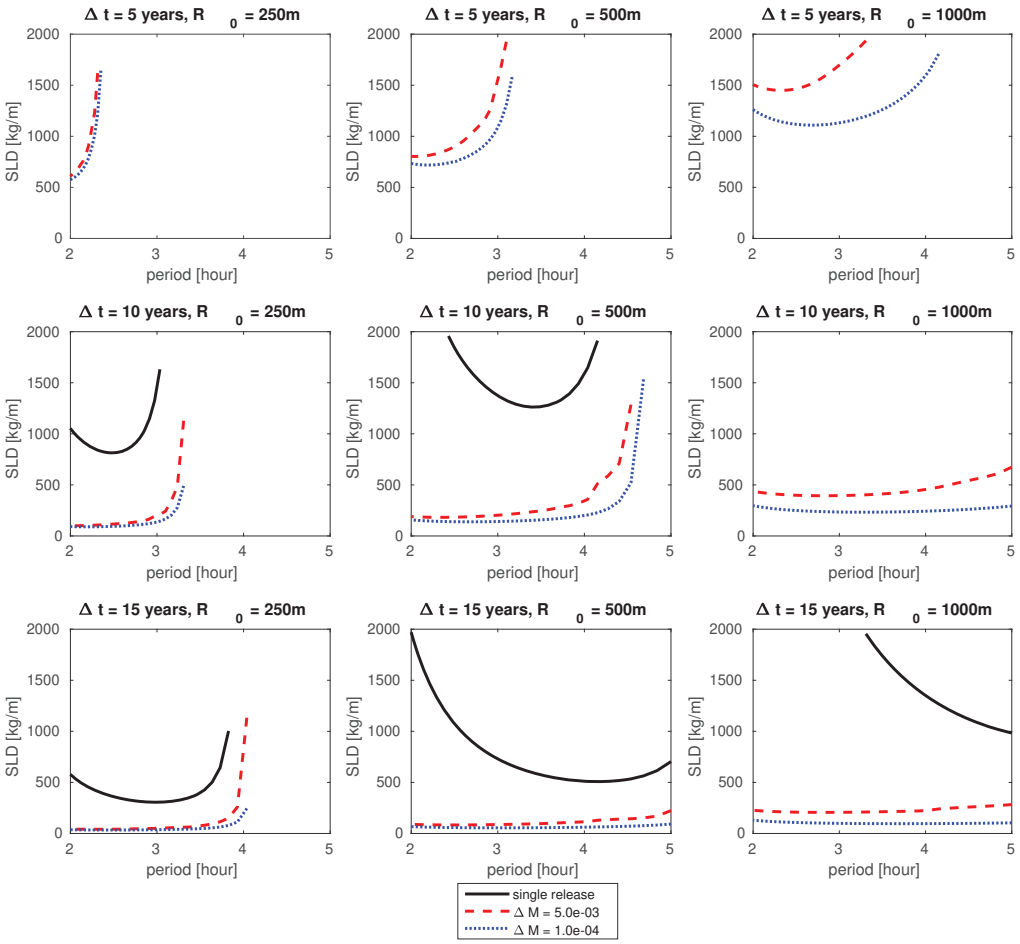

Fig. 16 Required siphon linear density to divert an asteroid by 1 Earth radius, for different asteroid radii and time windows.

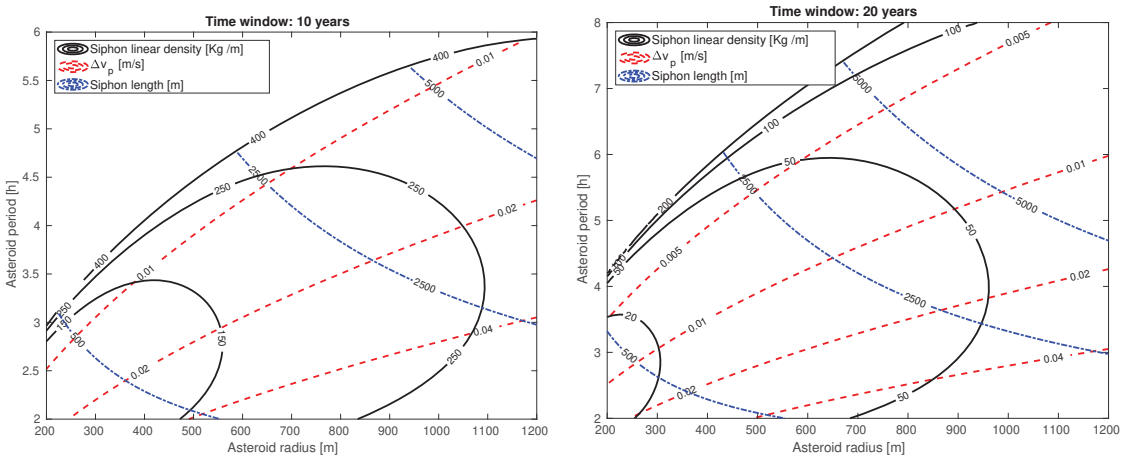

(a) (b)

Fig. 17 Isocurves for siphon linear density (black), Δv_p (red) and siphon length (blue) as a function of the asteroid radius and period, for a MR release scenario, with $\Delta\bar{m} = 1 \times 10^{-4}$ and asteroid density $\rho = 2\,\mathrm{g\,cm^{-3}}$.

as a function of the asteroid radius and period, combined with the isocurves of primary release velocity (red) and siphon length (blue), for a 10 (a) and 20 (b) years deflection. Note that regions with lower μ are also characterized by a smaller siphon length. Figure 17 clearly shows that smaller and fast rotating asteroids are preferred candidates for such deflection method, with smaller siphon linear density and siphon length requirements.

The siphon linear density is also related to the cross section of the siphon, with larger μ being associated to larger cross sections. In particular, the total mass of the siphon μL can be expressed as a function of the siphon cross section A as

$$\mu L = AL\rho \tag{54}$$

thus:

$$A = \frac{\mu}{\rho} \tag{55}$$

Then, $\sqrt{A}$ provides the width of the siphon, modelled as a continuous mass distribution with squared cross section. For siphon linear density ranging from 20 to 400 kg/m, $\sqrt{A}$ ranges from 10 cm to 45 cm. Nevertheless, a siphon modelled as a discrete chain of payloads will clearly have a larger cross section, depending on the distance λ between consecutive payloads. Assuming that payloads are stored within buckets of cubical shape, it can be shown that the size of the payloads is $\sqrt[3]{\mu\lambda/\rho}$, where, to avoid superposition of consecutive payloads, $\lambda \geq \sqrt{\mu/\rho}$. For example, taking a distance between payloads of $\lambda = 0.5\,\mathrm{m}$, for the same range of μ, the size of the payload ranges from 17 cm to 46 cm. The total number of payloads then depends on the length of the chain.

Table 2 Relevant dimensional parameters for the deflection of the asteroid 263976 (2009 KD5) (radius 393 m, period 2.66 hours) by 1 Earth radius in 10 and 20 years, using a MR strategy, with $\Delta\bar{m} = 1 \times 10^{-4}$.

		10 years	20 years
Siphon linear density	[kg/m]	118	24
Total Δv_p	[cm/s]	1.15	0.63
Average Δv_s	[cm/s]	60	54
Average mass rate	[kg/s]	34	8
Number of releases		214	106
Released mass	%	0.0213	0.0105
Siphon length	[m]	670	670
Max tension	[kN]	8.4	8.4

A. Case study and discussion

Table 2 shows relevant parameter in dimensional units, referred to the MR deflection of the potentially hazardous asteroid 263976 (2009 KD5) (radius 393 m, period 2.66 hours [†]) in 10 years and 20 years by 1 Earth radius, assuming an asteroid density $\rho = 2\,\mathrm{g\,cm^{-3}}$. Figure 18 also shows the trajectory in the CW frame for the 10 years deflection case. The siphon linear density drops by about one order of magnitude when the time windows is doubled. This implies a reduction of both the siphon cross section and the mass rate of material being lifted on the siphon, taken as the ratio between the total released mass and the time window. The required mass rates range from 8 to 34 $\mathrm{kg\,s^{-1}}$ for the scenario presented. Such rates clearly depend upon the technology of the mining units transferring material from the surface of the asteroid to the siphon and the physical properties of the asteroid. For example, surface irregularities, boulders or cavities might interfere with the motion of surface rovers. Furthermore, locomotion speeds of wheeled or hopping rovers are limited by the escape velocity of the asteroid, on the order of $17\,\mathrm{cm\,s^{-1}}$ for case presented. An efficient solution to this issue, as discussed in [18] is to use a tethered network of cables fixed on the asteroid surface, acting as a "railway" for rover locomotion. Rovers would use these tethered network to move at arbitrary speeds on the asteroid surface and quickly move between the mining location and the siphon base. Additionally, use of multiple siphons, anchored at different points on the asteroid equator, would significantly reduce the overall travel distance of surface rovers, thus enabling larger mass throughputs. In any case, the required mass flow rate significantly decreases for larger time windows or, in general, when the Δv decreases. In cases where an asteroid has a close approach to Earth followed by a later return, the required change in velocity needed may be orders of magnitude smaller than $1\,\mathrm{cm\,s^{-1}}$ [6], thus significantly reducing the required mass flow rate.

The maximum support tether tension is 8.4 kN in both cases. A Kevlar tether (density $1.44\,\mathrm{g\,cm^{-3}}$, maximum tensile strength 3.6 GPa [24]) with cross section of $1\,\mathrm{cm^2}$ can withstand such tension, with a total tether mass of approximately 10 kg. It must be stressed that the tether tension can vary significantly depending on the asteroid radius, period and the

[†]From, https://ssd.jpl.nasa.gov/sbdb.cgi, accessed on 14th May 2020

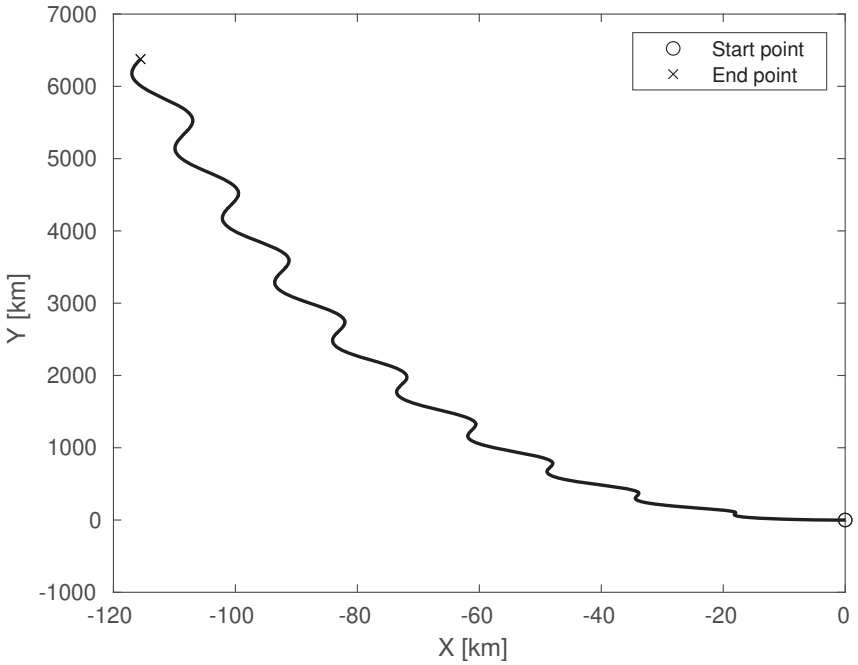

Fig. 18 Primary trajectory for a 10 years deflection of asteroid 263976 (2009 KD5) by 1 Earth radius.

released mass Δm. Therefore a range of very different scenarios and requirements might emerge depending on the asteroid physical characteristics.

The total released mass is approximately 2% and 1% of the asteroid initial mass for a 10 and 20 year deflection scenario respectively. This corresponds to about 5×10^6 and 1×10^7 tonnes of material. This reaction mass is much larger than that required by other deflection methods. However, it must be emphasized that the reaction mass is entirely collected *in situ* and that is one of the main advantages of the orbital siphon deflection method.

An estimate of the size of the buckets can be made using the equations described in the previous section. For example, assuming cubic buckets and 1 m distance between them, each cubic bucket would have a side length of approximately 39 cm for the 10 years deflection scenario and 23 centimeters for the 20 years deflection scenario. The mass of the buckets will depend on the selected material and the thickness of each bucket face. However, depending on the average grain size of the asteroid material, buckets can be designed as a wire mesh thus significantly decreasing their mass and therefore the siphon structural mass to be launched from Earth.

Typical secondary escape velocities are between 54 and 60 $\mathrm{cm\,s^{-1}}$, much larger than the total Δv of the primary. Considering the secular term only in the CW equations, the total secondary displacement in the time Δt is $3\Delta v_s \Delta t$. Therefore a secondary released with escape velocity $\Delta v_s = 54\,\mathrm{cm\,s^{-1}}$ would be displaced by about 8 Earth radii per year. It is therefore reasonable to assume that the secondaries will always miss Earth. More accurate analysis, taking into account orbital eccentricity and inclination, is left for future work.

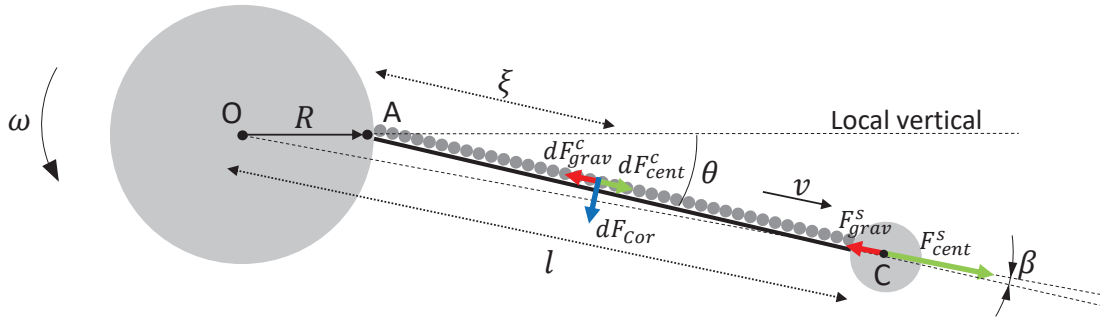

Fig. 19 Orbital siphon not aligned with the local vertical. Also shown are the forces acting on an element of mass of the chain and on the secondary.

V. Conclusion

Results from this preliminary analysis have demonstrated that the orbital siphon effect can be in principle exploited to deflect an asteroid by leveraging its rotational kinetic energy.

In particular, it has been shown that better performances are achieved when the asteroid mass is released in multiple small fractions, rather than a single release of a larger mass. This allows a reduction of the density of material being transported on the siphon and the tether tension for a given time window and diversion distance. A smaller siphon linear density implies a smaller siphon bulk mass and a smaller tension reduces the anchor force on the primary. The multiple mass release scenario also enables a reduction of the overall volume of the mass collected at the top of the siphon making the problem of handling the collected material easier. Secondly, although not directly considered here, the repeatability offered by the multiple release scheme offers more margin in case of errors in the release direction

Typical Δv on the order of 1 cm/s can be achieved in a time window of a decade, with siphon linear densities on the order of 100 kg/m. Larger Δv can be obtained for fast-rotators and larger asteroid, as they contain more rotational kinetic energy. However, the asteroid size has a direct impact on the time requirements, i.e., larger asteroids can be deflected by a larger Δv_p but within a longer time window.

A. Siphon alignment with local vertical

The purpose of this section is to show that, if the secondary mass is large enough, it is reasonable to assume that the siphon is aligned with the local vertical. Similar to Ref. [16], the idea is to evaluate the angular displacement of the siphon from the local vertical (the angle θ in Fig. 19), imposing the equilibrium of the torques acting on the siphon with respect to the anchor point on the primary, and to show that θ is small. Note that, if $\theta \neq 0$, the centrifugal-induced and gravitational forces acting on the chain and on the counterweight will generate a net torque with respect to the anchor point, due to the misalignment between the direction of those forces and the direction of the siphon (see Fig. 19). For simplicity it is assumed that $r \approx 0$, i.e., the secondary is treated as a point mass. [‡]. Also, the center-of-mass of the

[‡]Note that this is a conservative assumption. If $r > 0$ then the distance between the secondary and the anchor further increases, thus increasing the centrifugal-induced torque on the secondary (and also decreasing the gravitational torque in the opposite direction on the secondary), whereas the

system is here conservatively assumed to be coincident with the center-of-mass of the primary.

Assume that the angle θ between the siphon and the local vertical is not zero, as shown in Fig. 19 (with $\theta > 0$ in the configuration shown). The torque caused by the centrifugal-induced force acting on the secondary with respect to the anchor point on the primary can be written as:

$$T^s_{\text{cent}} = m\omega^2 l L \sin\beta \tag{56}$$

where l is the distance between the center-of-mass of the primary and the secondary whereas β is the angle between the segments OC and AC (see Fig. 19). Torques are considered positive when they induce a rotation in the same direction as the asteroid rotation. Similarly, the torque caused by the gravitational force acting on the secondary can be written as:

$$T^s_{\text{grav}} = -\frac{GM}{l^2} mL \sin\beta \tag{57}$$

The torque due to the centrifugal-induced forces acting on the chain can be found via the integral:

$$T^c_{\text{cent}} = \int_0^L \omega^2 \left(R^2 + \xi^2 + 2R\xi\cos\theta\right)^{1/2} \xi\mu \sin\beta d\xi \tag{58}$$

where ξ is the distance between the differential element of mass of the siphon and the anchor point A, found using the cosine theorem. Similarly, the torque due to the gravitational forces on the chain is given by

$$T^c_{\text{grav}} = -\int_0^L \frac{GM}{R^2 + \xi^2 + 2R\xi\cos\theta} \xi\mu \sin\beta d\xi \tag{59}$$

where the gravitational attraction between the chain and the secondary is conservatively neglected. Finally, the torque induced by the Coriolis forces is:

$$T_{\text{Cor}} = -\int_0^L 2\omega v \mu \xi d\xi \tag{60}$$

with v the radial velocity of the chain. The angle β can be written as a function of θ using the sine theorem applied to the triangle OAC

$$\frac{R}{\sin\beta} = \frac{l}{\sin\theta} \tag{61}$$

such that:

$$\sin\beta = \frac{R}{l}\sin\theta \tag{62}$$

Coriolis torque would remain unchanged, thus increasing θ_{eq} (Eq. (67))

Using the approximation $\theta \approx 0$, Eq. (62) can be written as:

$$\sin\beta \approx \beta = \frac{R}{R+L}\theta \tag{63}$$

where

$$l \approx R + L \tag{64}$$

Also, it is assumed that the siphon radial velocity for $\theta \approx 0$ is that given by Eq. (29) (the transitory effect is here conservatively not taken into account, hence the radial velocity is taken at its maximum value, which is the steady state $v = \sqrt{F/\mu}$). Substituting Eqs. (64) and (63) into Eqs. (56), (57),(58), (59), (60) and further simplifying yields:

$$T^s_{\text{cent}} = m\omega^2 LR\theta \tag{65a}$$

$$T^s_{\text{grav}} = -\frac{GM}{(R+L)^3} mRL\theta \tag{65b}$$

$$T^c_{\text{cent}} = \frac{1}{6}\omega^2 \frac{RL^2(2L+3R)}{R+L}\mu\theta \tag{65c}$$

$$T^c_{\text{grav}} = -GM\left(\ln\frac{L+R}{R} - \frac{L}{L+R}\right)\frac{R}{L+R}\mu\theta \tag{65d}$$

$$T_{\text{Cor}} = -\omega v L^2 \mu \tag{65e}$$

Under static conditions, the sum of all the toques with respect to the anchor point is zero:

$$T^s_{\text{cent}} + T^s_{\text{grav}} + T^c_{\text{cent}} + T^c_{\text{grav}} + T_{\text{Cor}} = 0 \tag{66}$$

Then, solving Eq. (66) for θ and further simplifying yields [§]:

$$\theta_{eq} = \frac{\dfrac{\bar{v}}{\bar{\omega} m^*}}{1 - \dfrac{1}{\bar{\omega}(1+\bar{L})^3} + \dfrac{1}{6}\dfrac{3+2\bar{L}}{1+\bar{L}}\dfrac{1}{m^*} - \left(\ln(1+\bar{L}) - \dfrac{\bar{L}}{1+\bar{L}}\right)\dfrac{1}{(1+\bar{L})\bar{L}^2}\dfrac{1}{\bar{\omega}^2 m^*}} \tag{67}$$

The angle θ_{eq} therefore represents the siphon angle θ at which all torques acting on the chain with respect to the anchor point are balanced. Note that θ_{eq} can be expressed as a function of the asteroid non-dimensional angular velocity $\bar{\omega}$, the siphon non-dimensional length $\bar{L}$ and $m^* = m/(\mu L)$ which is the mass of the secondary scaled with respect to the mass of the siphon [¶]. Figure 20 shows the equilibrium angle for a range of siphon lengths and angular velocities, and for $m^* = 50$ (a) and $m^* = 100$ (b). It is apparent that the equilibrium angle is on the order of 1 deg and, as expected, it decreases for a larger secondary mass. For example, for the candidate asteroid discussed in Sect. IV.A, using the

[§] Equation (67) can be easily obtained by dividing both sides of Eq. (66) by T^s_{cent} and then solving for θ

[¶] The asterisk superscript is used to distinguish the mass scale factor used here from the nominal mass scale factor used in the paper (Table 1).

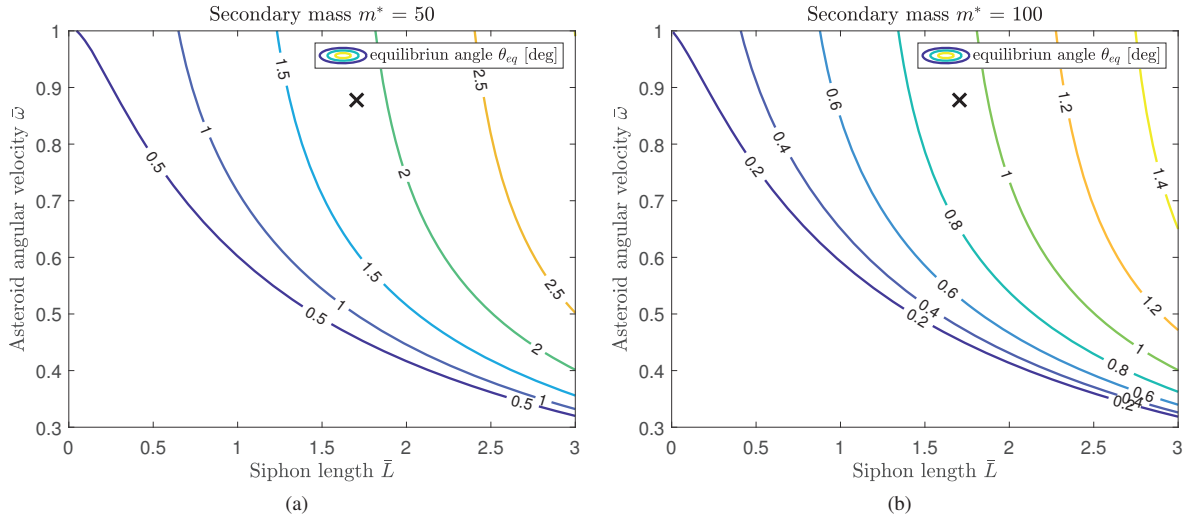

Fig. 20 Equilibrium angle θ_{eq} as a function of the non-dimensional siphon length $\bar{L}$ and the non-dimensional asteroid angular velocity $\bar{\omega}$, for two different values of the secondary mass scaled with respect to the mass of the siphon (m^*). The black cross represents the case for the candidate asteroid discussed in Sect. IV.A.

optimal siphon length for the primary deflection reported in Table 2, $\theta_{eq} = 1.85$ deg for $m^* = 50$ and $\theta_{eq} = 0.92$ deg for $m^* = 100$. Note that, if m^* is large then T^c_{cent} and T^c_{grav} become negligible with respect to the other terms and Eq. (67) admits the approximation

$$\theta_{eq} \approx \frac{\bar{\nu}}{m^*} \frac{1}{\bar{\omega} - \dfrac{1}{(1+\bar{L})^3}} \tag{68}$$

and so $\theta_{eq} \propto 1/m^*$. Therefore, for a large secondary mass, the equilibrium angle is well approximated by parameters depending only on T^s_{cent}, T^s_{grav} and T_{Cor}. To justify the assumption of alignment between the siphon and the local vertical it can therefore be assumed that part of the secondary mass is not used as reaction mass for the asteroid deflection but its retained on the secondary as counterweight mass, such that the centrifugal-induced torque acting on the secondary is always large enough to counteract the Coriolis torque due to the siphon effect.

Funding Sources

CM is supported by a Royal Academy of Engineering Chair in Engineering Technologies and a Royal Society Wolfson Research Merit Award.

References

[1] Elvis, M., "Let's mine asteroids for science and profit," *Nature*, Vol. 485, No. 7400, 2012, pp. 549–549. https://doi.org/10.1038/485549a.

[2] Sanchez, J. P., and Colombo, C., "Impact Hazard Protection Efficiency by a Small Kinetic Impactor," *Journal of Spacecraft and*

Rockets, Vol. 50, No. 2, 2013, pp. 380–393. https://doi.org/10.2514/1.a32304.

[3] McInnes, C. R., "Deflection of near-Earth asteroids by kinetic energy impacts from retrograde orbits," *Planetary and Space Science*, Vol. 52, No. 7, 2004, pp. 587–590.

[4] Wie, B., "Astrodynamic fundamentals for deflecting hazardous near-earth objects," *60th International Astronautical Congress, IAC-09-C1.3.1*, Vol. 3, 2009, pp. 12–16.

[5] Sagan, C., and Ostro, S. J., "Dangers of asteroid deflection," *Nature*, Vol. 368, No. 6471, 1994, pp. 501–501. https://doi.org/10.1038/368501a0.

[6] Lu, E. T., and Love, S. G., "Gravitational tractor for towing asteroids," *Nature*, Vol. 438, No. 7065, 2005, p. 177.

[7] Bombardelli, C., Urrutxua, H., Merino, M., Peláez, J., and Ahedo, E., "The ion beam shepherd: A new concept for asteroid deflection," *Acta Astronautica*, Vol. 90, No. 1, 2013, pp. 98–102. https://doi.org/10.1016/j.actaastro.2012.10.019, URL https://doi.org/10.1016%2Fj.actaastro.2012.10.019.

[8] Scheeres, D., and Schweickart, R., "The Mechanics of Moving Asteroids," 2004 Planetary Defense Conference: Protecting Earth from Asteroids, 2004. https://doi.org/10.2514/6.2004-1446.

[9] Spitale, J. N., "Asteroid hazard mitigation using the Yarkovsky effect," *Science*, Vol. 296, No. 5565, 2002, pp. 77–77. https://doi.org/10.1126/science.1069577.

[10] Ahrens, T. J., and Harris, A. W., "Deflection and fragmentation of near-Earth asteroids," *Nature*, Vol. 360, No. 6403, 1992, pp. 429–433. https://doi.org/10.1038/360429a0.

[11] Brack, D. N., and McMahon, J. W., "Dynamical Behavior of an Asteroid Undergoing Material Removal," *2018 Space Flight Mechanics Meeting*, American Institute of Aeronautics and Astronautics, 2018. https://doi.org/10.2514/6.2018-0954.

[12] French, D. B., and Mazzoleni, A. P., "Asteroid Diversion Using Long Tether and Ballast," *Journal of Spacecraft and Rockets*, Vol. 46, No. 3, 2009, pp. 645–661. https://doi.org/10.2514/1.40828.

[13] Mashayekhi, M., and Misra, A., "Tether assisted near earth object diversion," *Acta Astronautica*, Vol. 75, 2012, pp. 71–77. https://doi.org/10.1016/j.actaastro.2011.12.018.

[14] McInnes, C. R., and Davis, C., "Novel Payload Dynamics on Space Elevator Systems," *56th International Astronautical Congress, IAC-05-D4.2-07*, 2005. https://doi.org/10.2514/6.iac-05-d4.2.07.

[15] Viale, A., McInnes, C., and Ceriotti, M., "Analytical mechanics of asteroid disassembly using the Orbital Siphon effect," *Proceedings of the Royal Society A: Mathematical, Physical and Engineering Sciences*, Vol. 474, No. 2220, 2018, p. 20180594. https://doi.org/10.1098/rspa.2018.0594.

[16] Viale, A., Ceriotti, M., and McInnes, C., "Dynamics of an orbital siphon anchored to a rotating ellipsoidal asteroid for resource exploitation," *Acta Astronautica*, 2020. https://doi.org/10.1016/j.actaastro.2020.08.001, URL https://doi.org/10.1016%2Fj.actaastro.2020.08.001.

[17] Viale, A., McInnes, C. R., and Ceriotti, M., "Disassembly of Near Earth Asteroids by Leveraging Rotational Self Energy," *69th International Astronautical Congress, IAC-18-D4.3-18*, 2018. URL http://eprints.gla.ac.uk/168724/.

[18] Viale, A., McInnes, C., and Ceriotti, M., "Dynamics of a Nonrigid Orbital Siphon at a Near-Earth Asteroid," *Journal of Guidance, Control, and Dynamics*, 2020, pp. 1–15. https://doi.org/10.2514/1.g004894, URL https://doi.org/10.2514%2F1.g004894.

[19] Hintz, G. R., *Fundamentals of Astrodynamics*, Springer International Publishing, 2015. https://doi.org/10.1007/978-3-319-09444-1_1.

[20] Scheeres, D., Hartzell, C., Sánchez, P., and Swift, M., "Scaling forces to asteroid surfaces: The role of cohesion," *Icarus*, Vol. 210, No. 2, 2010, pp. 968–984. https://doi.org/10.1016/j.icarus.2010.07.009.

[21] Pravec, P., and Harris, A. W., "Fast and Slow Rotation of Asteroids," *Icarus*, Vol. 148, No. 1, 2000, pp. 12–20. https://doi.org/10.1006/icar.2000.6482.

[22] Clohessy, W., and Wiltshire, R., "Terminal guidance system for satellite rendezvous," *Journal of the Aerospace Sciences*, Vol. 27, No. 9, 1960, pp. 653–658. https://doi.org/https://doi.org/10.2514/8.8704.

[23] Cuartielles, J. P. S., Colombo, C., Vasile, M., and Radice, G., "A Multi-criteria Assessment of Deflection Methods for Dangerous NEOs," *AIP Conference Proceedings*, AIP, 2007. https://doi.org/10.1063/1.2710065.

[24] Aravind, P. K., "The physics of the space elevator," *American Journal of Physics*, Vol. 75, No. 2, 2007, pp. 125–130. https://doi.org/10.1119/1.2404957.